2022 2nd Season Stock Assessment

Falkland calamari

(*Doryteuthis gahi*)

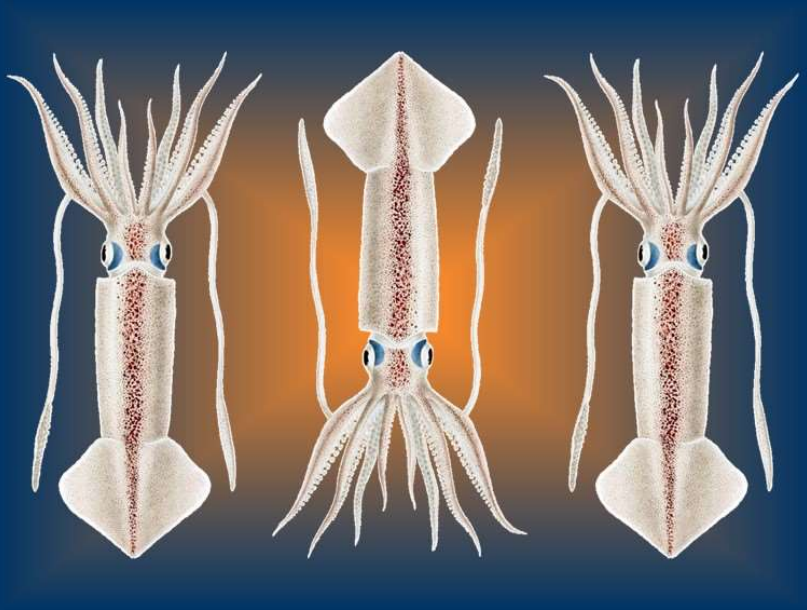

Andreas Winter · Frane Skeljo

Natural Resources - Fisheries
Falkland Islands Government
Stanley, Falkland Islands

November 2022

S2 - 2022 - LOL

Index

Summary

1) The 2022 second season *Doryteuthis gahi* fishery (X license) was open from July 28th and closed as planned on September 29th. Compensatory flex days resulted in thirty vessel-days, by fourteen vessels, taken after September 29th, with the last vessel fishing until October 3rd.
2) 43,216 tonnes of *D. gahi* catch was reported in the 2022 X-license fishery, giving an average CPUE of 44.0 t vessel-day^{-1}. Total catch and CPUE were the highest on record for second seasons, ahead of 40,539 tonnes in 1995 and 39.0 t vessel-day^{-1} in 2019. 67.3% of *D. gahi* catch and 55.6% of fishing effort were taken south of 52º S; 32.7% of *D. gahi* catch and 44.4% of fishing effort were taken north of 52º S.
3) In the south sub-area, three depletion periods / immigration peaks were inferred on July 28th (start of the season), August 3rd, and September 27th. In the north sub-area, three depletion periods / immigrations were inferred on July 28th, August 25th, and September 14th.
4) Approximately 45,428 tonnes of *D. gahi* (95% confidence interval: 37,113 to 71,013 t) were estimated to have immigrated into the Loligo Box after the start of second commercial season 2022, of which 22,506 t in the south sub-area and 22,923 t in the north sub-area.
5) The escapement biomass estimate for *D. gahi* remaining in the Loligo Box at the end of second season 2022 was: Maximum likelihood of 32,090 tonnes, with a 95% confidence interval of 26,920 to 73,086 tonnes.
   The risk of *D. gahi* escapement biomass at the end of the season being less than 10,000 tonnes was estimated at effectively zero.

Introduction

Second season (X licence) of the 2022 *Doryteuthis gahi* fishery (Patagonian longfin squid – colloquially *Loligo*) opened on July 28th, with 15 vessels entering the fishery. One vessel postponed its entry for a day due to delays with fuelling and equipping. Throughout the season, 33 compensatory days were requested by all except one vessel, of which 12 days on July 30th for bad weather and 15 on August 27th (Figure 1). A total of 30 fishing days were taken after scheduled closure on September 29th with the last vessel fishing on October 3rd.

All X-licensed vessels were required to embark a Marine Mammal Observer to monitor presence and incidental capture of pinnipeds, and as for the second Loligo season last year, seal exclusion devices (SEDs) were mandatory for the duration of the season. Ultimately, 20 pinniped mortalities were reported for the season: 17 South American fur seals *Arctocephalus australis*, 2 Southern sea lions *Otaria flavescens*, and 1 unidentified animal.

Total reported *D. gahi* catch under second season X licence was 29,082.3 south + 14,133.9 north = 43,216.2 tonnes, corresponding to an average CPUE of 43216 / 982 = 44.0 tonnes vessel-day^{-1}. Both total catch and average CPUE were highest on record for second seasons. The second-highest second season catch was 40538.5 tonnes in 1995 (taken over 1724 fishing days), and the second-highest second season average CPUE was 39.0 tonnes vessel-day^{-1} in 2019 (Table 1); a season closed early for stock conservation (Winter 2019).

Figure 1 [next page]. Fish Ops chart display (Big Ocean Data) (right) and wind speed vector plots (Copernicus Marine Service) (left) on July 30th, when only four vessels fished, and August 27th, when only one vessel fished.

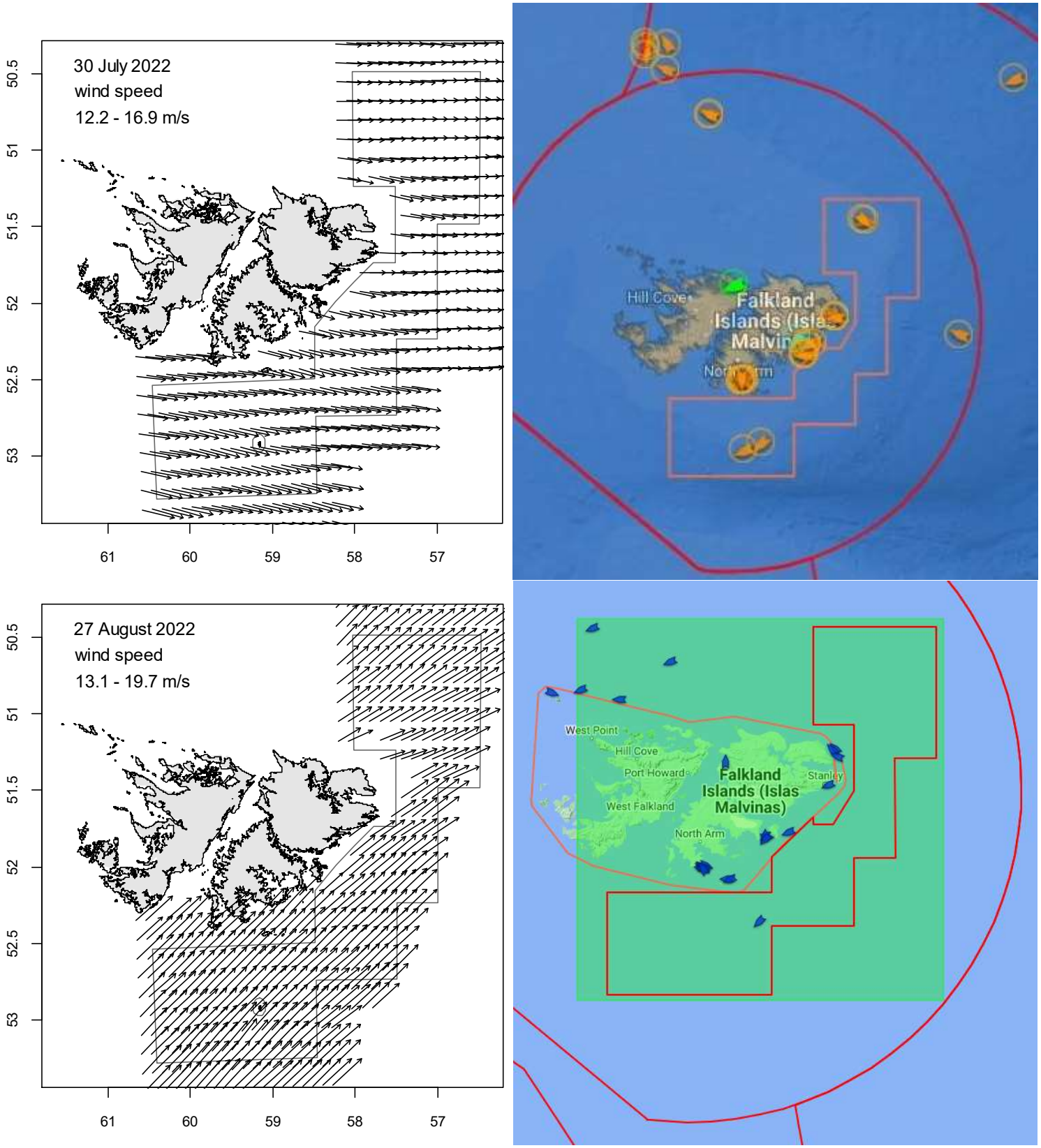

Assessment of the Falkland Islands *D. gahi* stock was conducted with depletion time-series models as in previous seasons (Agnew et al. 1998, Roa-Ureta and Arkhipkin 2007, Arkhipkin et al. 2008), and in other squid fisheries (cited in Arkhipkin et al. 2021). Because *D.*

gahi has an annual life cycle (Patterson 1988, Arkhipkin 1993), stock cannot be derived from a standing biomass carried over from prior years (Rosenberg et al. 1990, Pierce and Guerra 1994). The depletion model instead calculates an estimate of population abundance over time by evaluating what levels of abundance and catchability must be present to sustain the observed rate of catch. Depletion modelling of the *D. gahi* target fishery is used in-season, for projection, and for post-season analysis, with the objective of maintaining an escapement biomass of 10,000 tonnes *D. gahi* at the end of each season as a conservation threshold (Agnew et al. 2002, Barton 2002).

Table 1. *D. gahi* season comparisons since 2004, when catch management was assumed by the FIFD. Days: total number of calendar days open to licensed *D. gahi* fishing including (since 1st season 2013) optional flex days; V-Days: aggregate number of licensed *D. gahi* fishing days reported by all vessels for the season. Entries in italics are seasons closed by emergency order.

	Season 1			Season 2		
	Catch (t)	Days	V-Days	Catch (t)	Days	V-Days
2004	7,152	46	625	17,559	78	1271
2005	24,605	45	576	29,659	78	1210
2006	19,056	50	704	*23,238*	*53*	*883*
2007	17,229	50	680	*24,171*	*63*	*1063*
2008	24,752	51	780	26,996	78	1189
2009	12,764	50	773	*17,836*	*59*	*923*
2010	28,754	50	765	36,993	78	1169
2011	15,271	50	771	*18,725*	*70*	*1099*
2012	34,767	51	770	35,026	78	1095
2013	19,908	53	782	19,614	78	1195
2014	28,119	59	872	19,630	71	1099
2015	*19,383*	*57*	*871*[A]	*10,190*	*42*	*665*
2016	22,616	68	1020	23,089	68	1004
2017	39,433	68	999[B]	24,101	69	1002[C]
2018	43,085	69	975	35,828	68	977
2019	55,586	68	953	*24,748*	*43*	*635*
2020	29,116	68	1012	29,759	69	993
2021	*59,587*	*62*	*891*	34,750	68	982[D]
2022	56,417	68	966[E]	43,216	68	982

[A] Does not include C-license catch or effort after the target was switched from *D. gahi* to *Illex*.
[B] Includes two vessel-days of experimental fishing for juvenile toothfish.
[C] Includes one vessel-day of experimental fishing for juvenile toothfish.
[D] Includes three vessel-days of experimental fishing for SED improvement.
[E] Includes three vessel-days of exploratory fishing north of the Loligo Box.

Methods

The depletion model formulated for the Falklands *D. gahi* stock is based on the equivalence:

$$C_{day} = q \times E_{day} \times N_{day} \times e^{-M/2} \quad \textbf{(1)}$$

where q is the catchability coefficient, M is the natural mortality rate (considered constant at 0.0133 day^{-1}; Roa-Ureta and Arkhipkin 2007), and C_{day}, E_{day}, N_{day} are respectively catch (numbers of squid), fishing effort (numbers of vessels), and abundance (numbers of squid) per

day. The catchability coefficient q summarized the range of variation of all trawls taken by the fishing fleet in this season.

In its basic form (DeLury 1947) the depletion model assumes a closed population in a fixed area for the duration of the assessment. However, the assumption of a closed population is imperfectly met in the Falkland Islands fishery, where stock analyses have often shown that *D. gahi* groups arrive in successive waves after the start of the season (Roa-Ureta 2012, Winter and Arkhipkin 2015). Arrivals of successive groups are inferred from discontinuities in the catch data. Fishing on a single, closed cohort would be expected to yield gradually decreasing CPUE, but gradually increasing average individual sizes, as the squid grow. When instead these data change suddenly, or in contrast to expectation, the immigration of a new group to the population is indicated (Winter and Arkhipkin 2015).

In the event of a new group arrival, the depletion calculation must be modified to account for this influx. Modification is done using a simultaneous algorithm that adds new arrivals on top of the stock previously present, and posits a common catchability coefficient for the entire depletion time-series. If two depletions are included in the same model (i.e., the stock present from the start plus a new group arrival), then:

$$C_{day} = q \times E_{day} \times (N1_{day} + (N2_{day} \times i2|_0^1)) \times e^{-M/2} \quad \textbf{(2)}$$

where i2 is a dummy variable taking the values 0 or 1 if 'day' is before or after the start day of the second depletion. For more than two depletions, $N3_{day}$, i3, $N4_{day}$, i4, etc., would be included following the same pattern.

The season depletion likelihood function was calculated as the difference between actual catch numbers reported and catch numbers predicted from the model (Equation **2**), statistically corrected by a factor relating to the number of days of the depletion period (Roa-Ureta 2012):

$$\text{minimization} \rightarrow \ ((n\text{Days} - 2)/2) \times \log\left(\sum_{days}\left(\log(\text{predicted } C_{day}) - \log(\text{actual } C_{day})\right)^2\right) \quad \textbf{(3)}$$

The stock assessment was set in a Bayesian framework (Punt and Hilborn 1997), whereby results of the season depletion model are conditioned by prior information on the stock; in this case the information from the pre-season survey.

The likelihood function of prior information was calculated as the normal distribution of the difference between catchability derived from the survey abundance estimate ($_{prior}q$), and catchability derived from the season depletion model ($_{depletion}q$). Applying this difference requires both the survey and the season to be fishing the same stock with the same gear. Catchability, rather than abundance N, is used for calculating prior likelihood because catchability informs the entire season time series; whereas N from the survey only informs the first in-season depletion period – subsequent immigrations and depletions are independent of the abundance that was present during the survey. Thus, the prior likelihood function was:

$$\text{minimization} \rightarrow \ \frac{1}{\sqrt{2\pi \cdot SD_{prior\ q}{}^2}} \times \exp\left(-\frac{\left({}_{depletion}q - {}_{prior}q\right)^2}{2 \cdot SD_{prior\ q}{}^2}\right) \quad \textbf{(4)}$$

where the standard deviation of catchability prior ($SD_{prior\ q}$) was calculated from the Euclidean sum (Carlson 2014) of the survey prior estimate uncertainty, the variability in catches on the

season start date, and the uncertainty in the natural mortality M estimate over the number of days mortality discounting (Appendix Equation **A5**).

Bayesian optimization of the depletion was calculated by jointly minimizing Equations **3** and **4**, using the Nelder-Mead algorithm in R programming package 'optimx' (Nash and Varadhan 2011). Relative weights in the joint optimization were assigned to Equations **3** and **4** as the converse of their coefficients of variation (CV), i.e., the CV of the prior became the weight of the depletion model and the CV of the depletion model became the weight of the prior. Calculations of the depletion CVs are described in Equations **A8-S** and **A8-N**. Because a complex model with multiple depletions may converge on a local minimum rather than global minimum, the optimization was stabilized by running a feed-back loop that set the q and N parameter outputs of the Bayesian joint optimization back into the in-season-only minimization (Equation **3**), re-calculated the in-season-only minimization, then re-calculated the Bayesian joint optimization, and continued this process until both the in-season minimization and the joint optimization remained unchanged.

With actual C_{day}, E_{day} and M being fixed parameters, the optimization of Equation **2** using Equations **3** and **4** produces estimates of q and N1, N2, …, etc. Numbers of squid on the final day (or any other day) of a time series are then calculated as the numbers N of the depletion start days discounted for natural mortality during the intervening period, and subtracting cumulative catch also discounted for natural mortality (CNMD). Taking for example a two-depletion period:

$$\begin{aligned} N_{\text{final day}} &= N1_{\text{start day 1}} \times e^{-M\,(\text{final day} - \text{start day 1})} \\ &+ N2_{\text{start day 2}} \times e^{-M\,(\text{final day} - \text{start day 2})} \\ &- CNMD_{\text{final day}}, \end{aligned} \quad \textbf{(5)}$$

$$CNMD_{\text{day 1}} = 0$$

$$CNMD_{\text{day x}} = CNMD_{\text{day x-1}} \times e^{-M} + C_{\text{day x-1}} \times e^{-M/2} \quad \textbf{(6)}$$

$N_{\text{final day}}$ is then multiplied by the average individual weight of squid on the final day to give biomass. Daily average individual weight is obtained from length / weight conversion of mantle lengths measured in-season by observers, and also derived from in-season commercial data as the proportion of product weight that vessels reported per market size category[a]. Observer mantle lengths are scientifically more accurate, but restricted to a partial sample of trawls. Commercially proportioned mantle lengths are relatively less accurate, but cover every trawl of the entire fishing fleet every day. Therefore, both sources of data are used (see Appendix – *Doryteuthis gahi* individual weights).

Distributions of the likelihood estimates from joint optimization (i.e., measures of their statistical uncertainty) were computed using a Markov Chain Monte Carlo (MCMC) (Gamerman and Lopes 2006), a method that is commonly employed for fisheries assessments (Magnusson et al. 2013). MCMC is an iterative process which generates random stepwise changes to the proposed outcome of a model (in this case, the q and N of *D. gahi* squid) and at each step, accepts or nullifies the change with a probability equivalent to how well the change fits the model parameters compared to the previous step. The resulting sequence of accepted or nullified changes (i.e., the 'chain') approximates the likelihood distribution of the model outcome. The MCMC of the depletion models were run for 200,000 iterations; the first 1000 iterations were discarded as burn-in sections (initial phases over which the algorithm stabilizes); and the chains were thinned by a factor equivalent to the maximum of either 5 or

[a] First reported for Falkland Islands *D. gahi* by Payá (2006). Also used in some finfish commercial fisheries, see Plet-Hansen et al. 2018.

the inverse of the acceptance rate (e.g., if the acceptance rate was 12.5%, then every eighth (0.125^{-1}) iteration was retained) to reduce serial correlation. For each model three chains were run; one chain initiated with the parameter values obtained from the joint optimization of Equations **3** and **4**, one chain initiated with these parameters ×2, and one chain initiated with these parameters ×¼. Convergence of the three chains was accepted if the variance among chains was less than 10% higher than the variance within chains (Brooks and Gelman 1998). When convergence was satisfied the three chains were combined as one final set. Equations **5**, **6**, and the multiplication by average individual weight were applied to the CNMD and to each iteration of N values in the final set, and the biomass outcomes from these calculations represent the distribution of the estimate.

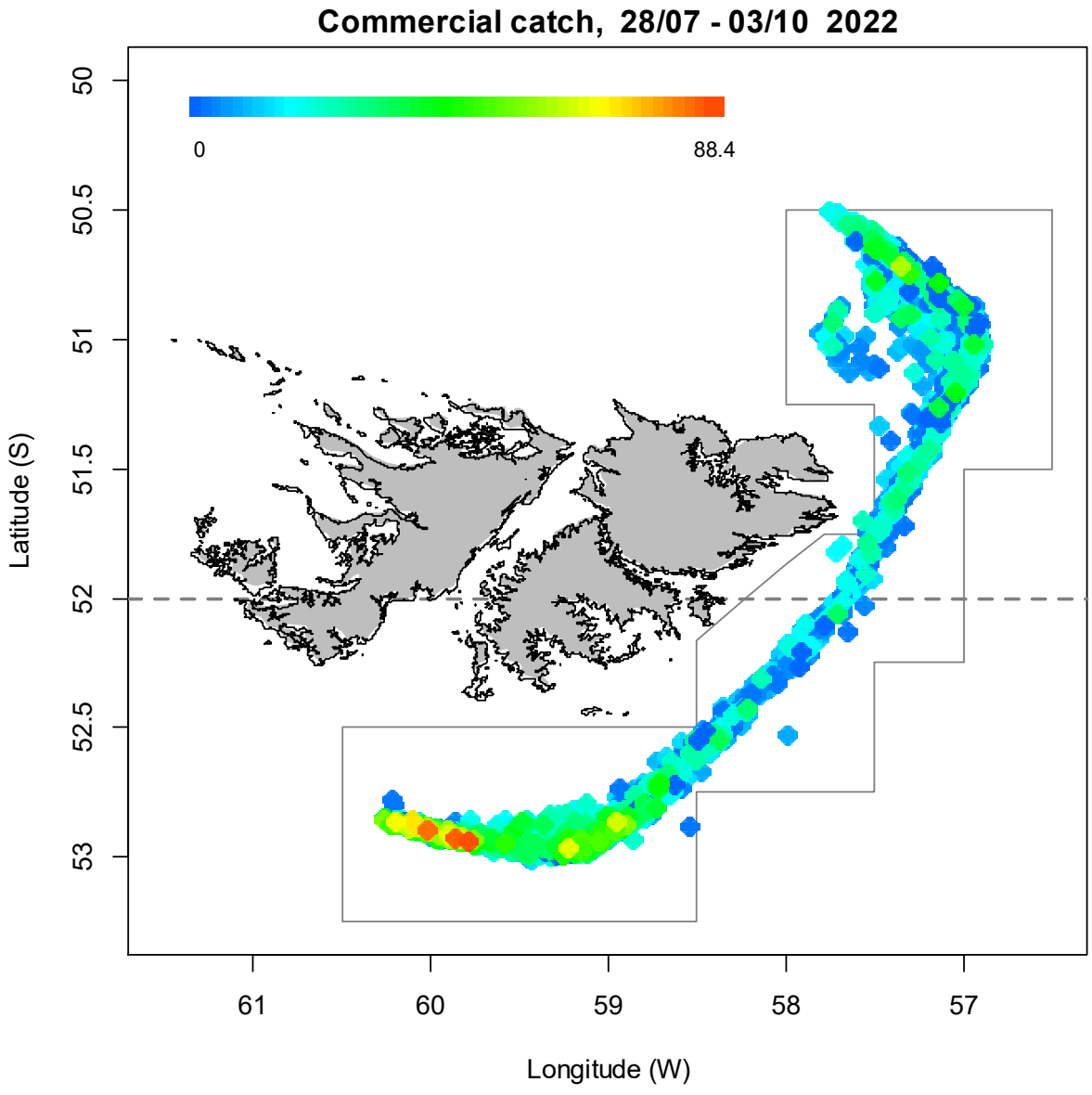

Figure 2. Spatial distribution of *D. gahi* 2nd-season trawls, colour-scaled to catch weight (max. = 88.4 tonnes). 2789 trawl catches were taken during the season. The Loligo Box fishing zone and 52 ºS parallel delineating the boundary between north and south assessment sub-areas, are shown in grey.

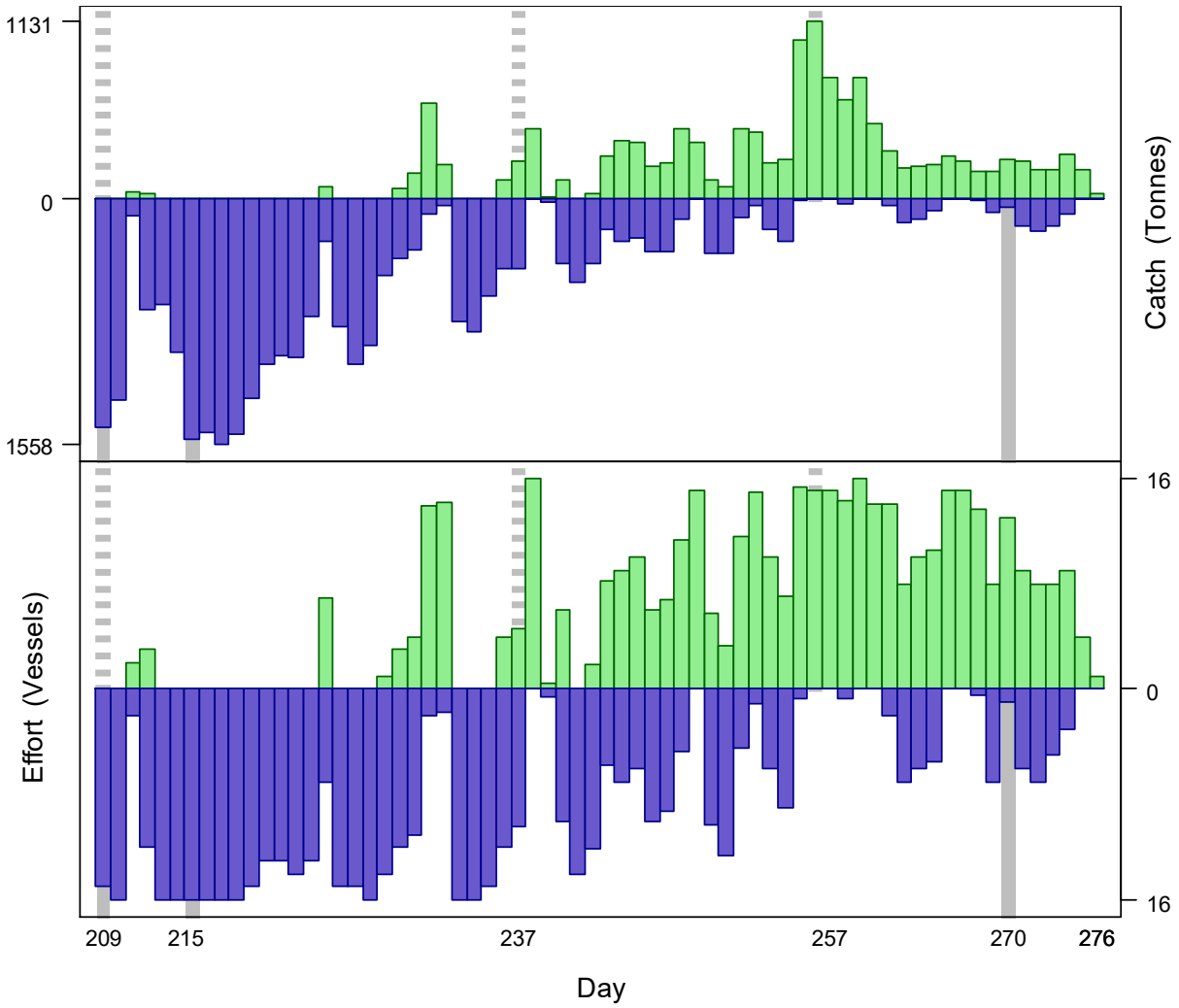

Figure 3. Daily total *D. gahi* catch and effort distribution by assessment sub-area north (green) and south (purple) of the 52º S parallel during 2nd season 2022. The season was open from July 28th (chronological day 209) with directed closure on September 29th (day 272), and flex days until October 3rd (day 276). As many as 16 vessels fished per day north; as many as 16 vessels fished per day south. As much as 1131 tonnes *D. gahi* was caught per day north; as much as 1558 tonnes *D. gahi* was caught per day south.

Depletion models and likelihood distributions were calculated separately for north and south sub-areas of the Loligo Box fishing zone, as *D. gahi* sub-stocks emigrate from different spawning grounds and remain to an extent segregated (Arkhipkin and Middleton 2002), although they represent a single intermixed population (Shaw et al. 2004). However, q_{prior} was calculated for the north and south sub-areas combined, rather than separately (Equation **A4**). As fishing tends to start predominantly in one or the other sub-area, rather than the fleet spreading itself evenly, separately computed north and south qs_{prior} are susceptible to arbitrary differences. Total escapement biomass was then defined as the aggregate biomass of *D. gahi* on the last day of the season for north and south sub-areas combined, with north and south likelihood distributions added together randomly.

For in-season analysis and management, the depletion model was implemented to calculate forward projections of the *D. gahi* biomass over periods of 7-10 days, that could be used to advise fishing companies of potential emergency closures of the season for stock

conservation. The procedure for calculating biomass forward projections is described in the Appendix – Biomass projection.

Stock assessment

Catch and effort

The north sub-area was fished on 48 of 68 season-days, for 32.7% of total catch (14133.9 tonnes *D. gahi*) and 44.4% of effort (435.5 vessel-days) (Figures 2 and 3). The south sub-area was fished on 58 of the 68 season-days, for 67.3% of total catch (29082.3 t *D. gahi*) – just above median percentage for second seasons – and 55.6% of effort (546.5 vessel-days) – the lowest second season percentage since 2017.

Data

982 vessel-days were fished during the season (Table 1), with a median of 15 vessels per day (mean 14.44). Vessels reported daily catch totals to the FIFD and electronic logbook data that included trawl times, positions, depths, and product weight by market size categories. Three FIG fishery observers were deployed on four vessels in the fishing season for a total of 55 sampling days[b] (Matosevic 2022a, b, Copping 2022, Sadd 2022). Throughout the 68 days of the season, 17 days had no FIG fishery observer sampling, 47 days had 1 FIG fishery observer sampling, and 4 days had two FIG fishery observers sampling. Except for seabird days FIG fishery observers were tasked with sampling 200 *D. gahi* at two stations daily; reporting their maturity stages, sex, and lengths to 0.5 cm. Contract marine mammal observers were tasked with measuring 200 unsexed lengths of *D. gahi* per day. The length-weight relationship for converting observer and commercially proportioned lengths was combined from second pre-season and season length-weight data of both 2021 and 2022, as 2022 data became available progressively with on-going observer coverage. The final parameterization of the length-weight relationship included 5379 measures from 2021 and 4680 measures from 2022, giving:

$$\text{weight (kg)} = 0.20484 \times \text{length (cm)}^{2.12999} / 1000 \quad \textbf{(7)}$$

with a coefficient of determination $R^2 = 91.7\%$.

Group arrivals / depletion criteria

Start days of depletions - following arrivals of new *D. gahi* groups - were judged primarily by daily changes in CPUE, with additional information from sex proportions, maturity, and average individual squid sizes. CPUE was calculated as metric tonnes of *D. gahi* caught per vessel per day. Days were used rather than trawl hours as the basic unit of effort. Commercial vessels do not trawl standardized duration hours, but rather durations that best suit their daily processing requirements. An effort index of days is therefore more consistent (FIFD 2004, Winter and Arkhipkin 2015). Inclusion of additional depletion starts was partially evaluated by improvement of the Akaike information criterion (Akaike 1973) on model fit. However, when the model is used for in-season monitoring, a new depletion start will almost certainly give a poorer AIC until a number of days have passed for better fit to supersede the penalty of the additional parameter. Improvement was therefore defined as showing a trend towards relatively

[b] Not counting seabird days (every fourth day).

lower AIC over progressive days rather than necessarily an outright lower AIC, so that depletion starts could be included as soon as their relevance was evident, and align the in-season model as soon as possible with the final post-season model.

Three days south and three days north were identified that represented the onset of significant immigrations / depletions throughout the season. The uneven early-season time series of catches and effort in the north (Figure 4) resulted in two additional days being evaluated, but ultimately did not meet criteria for substantiated influence on the depletion model. The last two days of fishing in the north also had high CPUE peaks, but were considered 'fill-up' catches by the few remaining vessels and not further immigration events.

- The first depletion start south was set by definition on day 209 (July 28th), the first day of the season with fifteen vessels fishing south. Average maturities were on that day near the lowest of the season (Figure 5D), and CPUE was near maximum (Figure 4).
- The second depletion start south was identified on day 215 (August 3rd), as CPUE increased to a high peak following several days of low catches (Figure 4). Average individual observer weights increased to a local maximum (Figure 5B).
- The third depletion start south was identified on day 270 (September 27th), on a day that only one vessel was fishing south, but showing a distinct local minimum of average individual observer weight (Figure 5B) along with a CPUE peak (Figure 4).
- The first depletion start north was set by definition on day 209 (July 28th), although no fishing in the north occurred until two days later. Average maturities prior to day 209 were the lowest of the season (Figure 5D).
- The second depletion start north was identified on day 237 (August 25th), with a peak in CPUE (Figure 4) and local minimum in average individual commercial weight (Figure 5A).
- The third depletion start north was identified on day 257 (September 14th) with the highest CPUE north of the season (Figure 4) and a distinct peak in the proportion of females (Figure 5C).

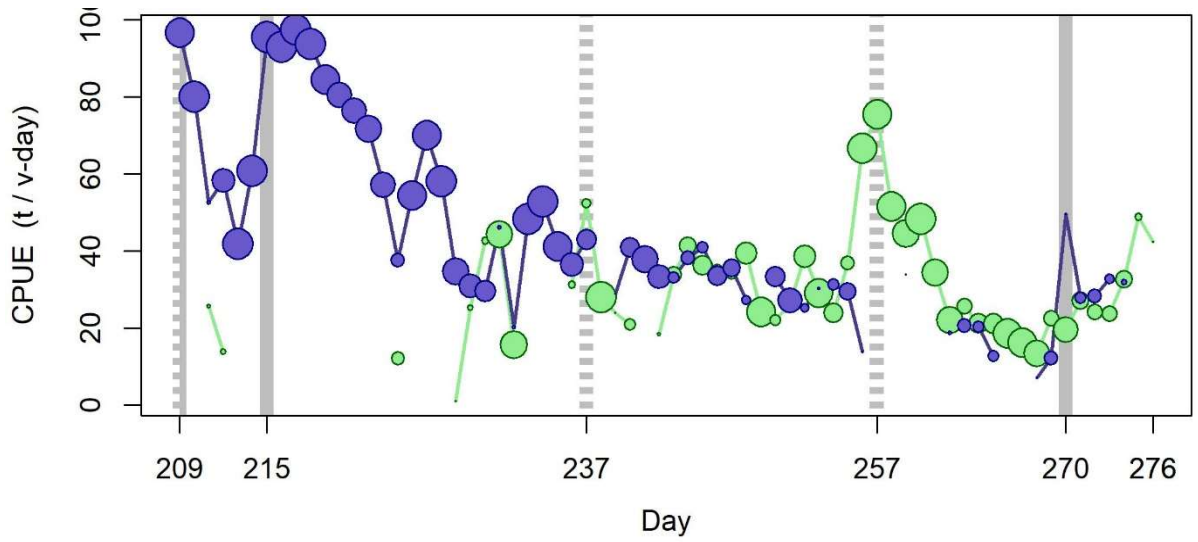

Figure 4. CPUE in metric tonnes per vessel per day, by assessment sub-area north (green) and south (purple) of 52º S latitude. Circle sizes are proportioned to numbers of vessels fishing. Data from consecutive days are joined by line segments. Broken grey bars indicate the starts of in-season depletions north. Solid grey bars indicate the starts of in-season depletions south.

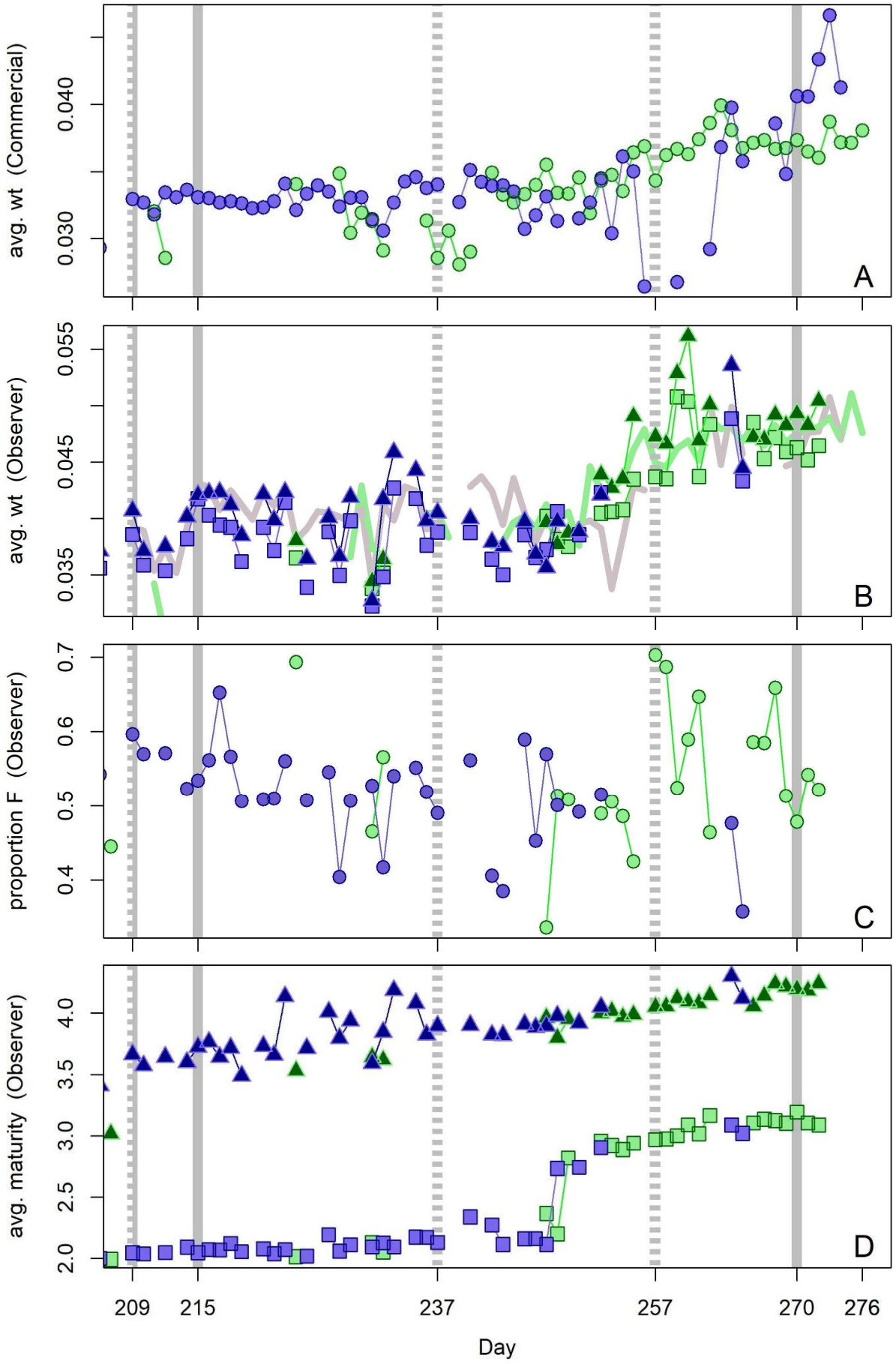
avg. wt (Commercial)
0.030
0.040
A
avg. wt (Observer)
0.035
0.045
0.055
B
proportion F (Observer)
0.4
0.5
0.6
0.7
C
avg. maturity (Observer)
2.0
2.5
3.0
3.5
4.0
D
209
215
237
257
270
276
Day

Figure 5 [previous page]. A: Average individual *D. gahi* weights (kg) per day from commercial size categories. B: Average individual *D. gahi* weights (kg) by sex per day from FIG observer sampling. C: Proportions of female *D. gahi* per day from observer sampling. D: Average maturity index value (Lipiński 1979) by sex per day from observer sampling. Males: triangles, females: squares, combined: circles. Thick lines (B) are unsexed measurements from the contract marine mammal observers. North sub-area: green, south sub-area: purple. Data from consecutive days are joined by line segments. Broken grey bars: starts of in-season depletions north. Solid grey bars: starts of in-season depletions south.

Depletion analyses
South

In the south sub-area, the maximum likelihood posterior ($_{Bayesian}\ q_S = 2.043 \times 10^{-3}$; Figure 6-left, and Equation **A9-S**) was preponderantly optimized on the in-season depletion ($_{depletion}\ q_S = 2.190 \times 10^{-3}$; Figure 6-left, and **A6-S**), which had 4.4× higher weight than the prior ($_{prior}\ q = 1.493 \times 10^{-3}$; Figure 6-left, and Equation **A4**) in the Bayesian model (Equations **A5** and **A8-S**).

The MCMC distribution of the Bayesian posterior multiplied by the generalized additive model (GAM) fit of average individual squid weight (Figure A1-south) gave the likelihood distribution of *D. gahi* biomass on day 276 (October 3rd) shown in Figure 6-right, with maximum likelihood and 95% confidence interval of:

$$B_{S\ day\ 276} = 15{,}685\ t \sim 95\%\ CI\ [11{,}855 – 25{,}223]\ t \qquad \textbf{(8-S)}$$

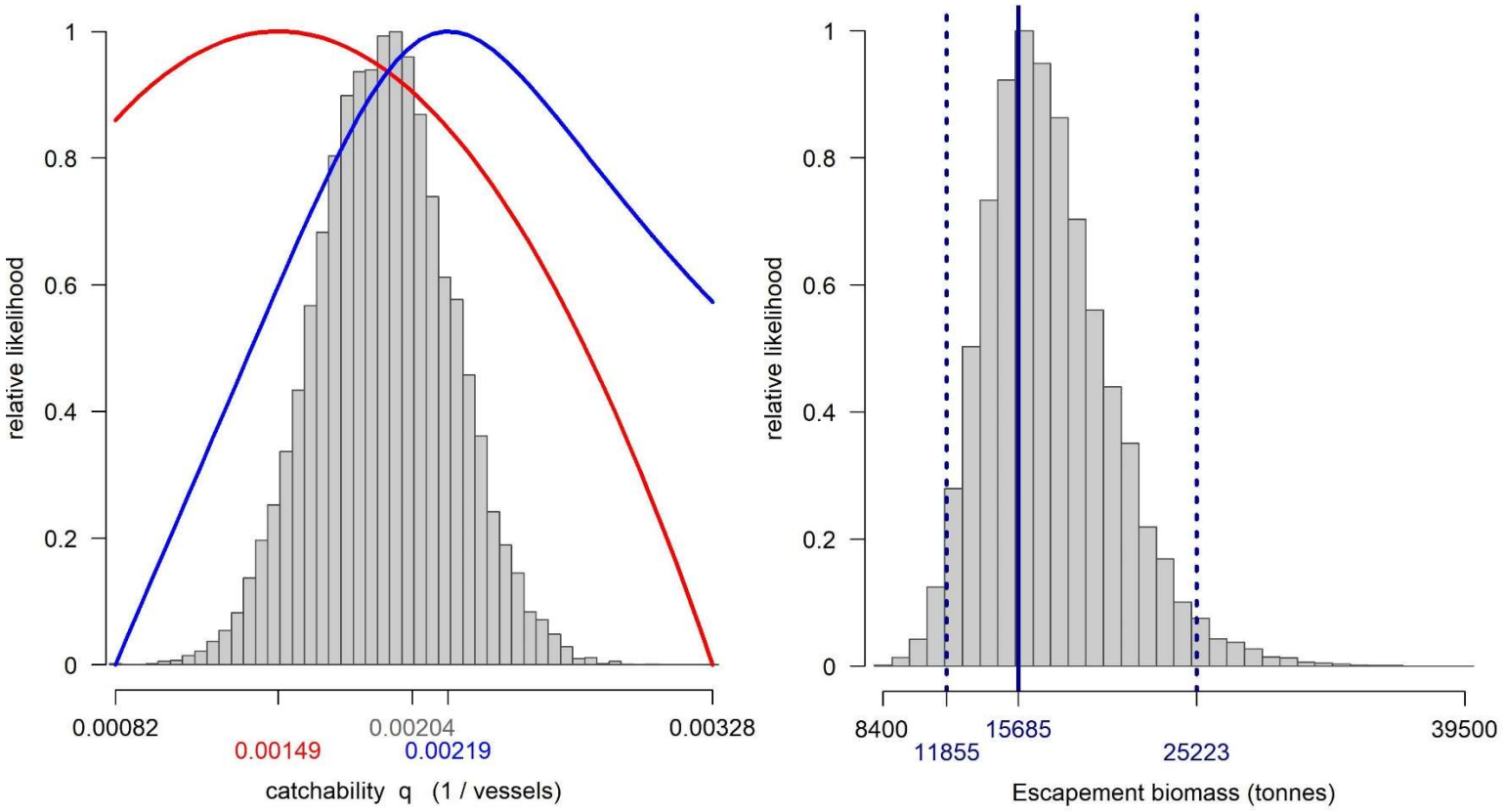

Figure 6 [previous page]. South sub-area. Left: Likelihood distributions for *D. gahi* catchability. Red line: prior model (pre-season survey data), blue line: in-season depletion model, grey bars: combined Bayesian model posterior. Right: Likelihood distribution (grey bars) of escapement biomass, from Bayesian posterior and average individual squid weight at the end of the season. Blue lines: maximum likelihood and 95% confidence interval. Note correspondence to Figure 7.

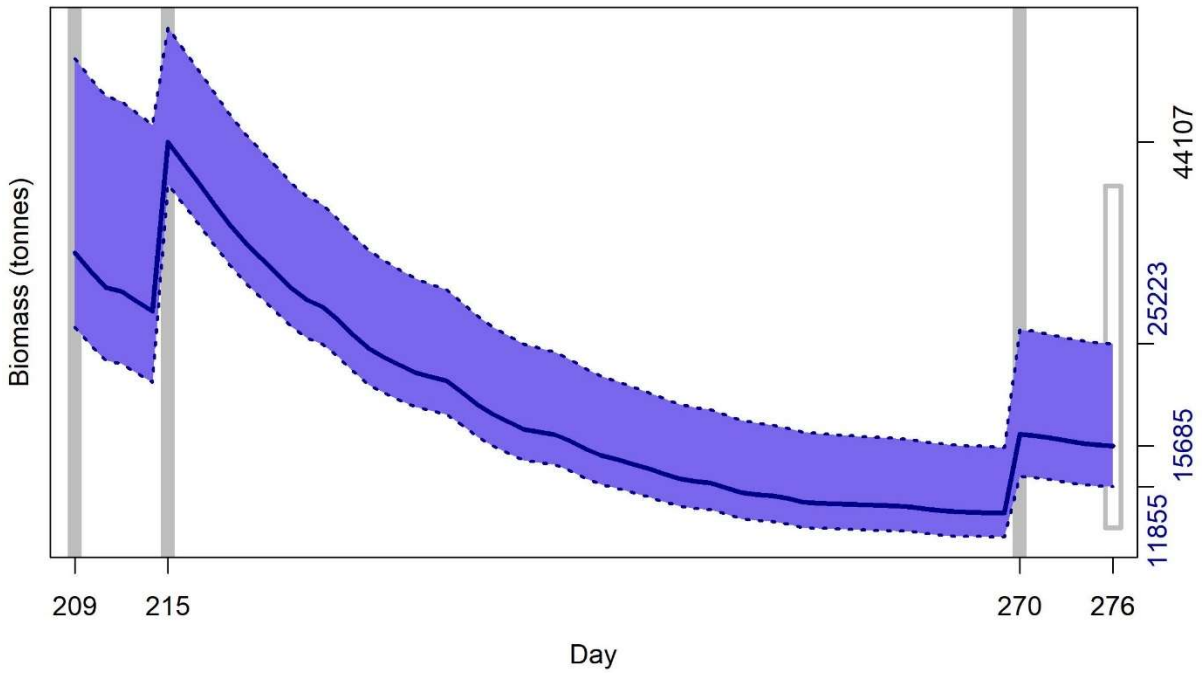

Figure 7. South sub-area. *D. gahi* biomass time series estimated from Bayesian posterior of the depletion model ± 95% confidence interval. Grey bars indicate the start of in-season depletions south; days 209, 215 and 270. Note that the biomass 'footprint' on day 276 (October 3rd) corresponds to the right-side plot of Figure 6.

On the first day of the season estimated *D. gahi* biomass south was 33,743 t ~ 95% CI [26,800 – 51,934] t (Figure 7); not statistically different from the pre-season estimate of 34,952 t [26,750 – 52,206] (Winter et al. 2022). The highest biomass estimate of the season occurred with the second immigration on day 215, reaching 44,107 t [40,169 – 54,865].

North

In the north sub-area, the maximum likelihood posterior ($_{\text{Bayesian}}\, q_N = 1.412 \times 10^{-3}$; Figure 8-left, and Equation **A9-N**) was preponderantly optimized on the prior ($_{\text{prior}}\, q = 1.493 \times 10^{-3}$; Figure 8-left, and Equation **A4**). The in-season depletion ($_{\text{depletion}}\, q_N = 0.463 \times 10^{-3}$; Figure 8-left, and Equation **A6-N**) had higher weight (lower CV) than the prior in the Bayesian model (Equations **A5** and **A8-N**), but by only a factor of approximately 1.6:1, given the relatively data-poor time series in the north (Figure 4).

The MCMC distribution plus average individual weight variation gave the likelihood distribution of *D. gahi* biomass on day 276 (October 3rd) shown in Figure 8-right, with maximum likelihood and 95% confidence interval of:

$$B_{N\ \text{day}\ 276} = 16{,}619\ \text{t} \sim 95\%\ \text{CI}\ [11{,}809 – 55{,}608]\ \text{t} \qquad \textbf{(8-N)}$$

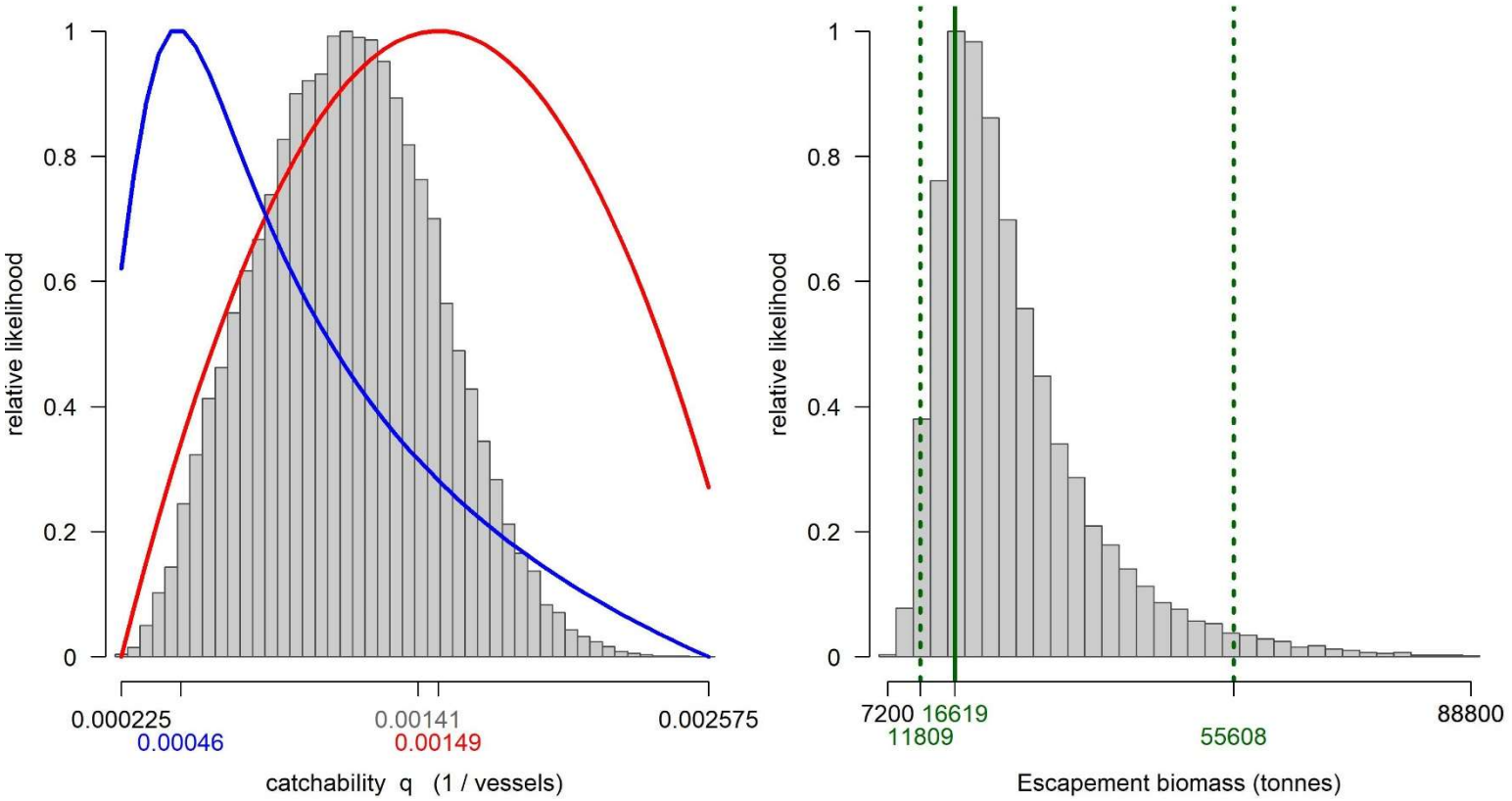

Figure 8. North sub-area. Left: Likelihood distributions for *D. gahi* catchability. Red line: prior model (pre-season survey data), blue line: in-season depletion model, grey bars: combined Bayesian model posterior. Right: Likelihood distribution (grey bars) of escapement biomass, from Bayesian posterior and average individual squid weight at the end of the season. Green lines: maximum likelihood and 95% confidence interval. Note the correspondence to Figure 9.

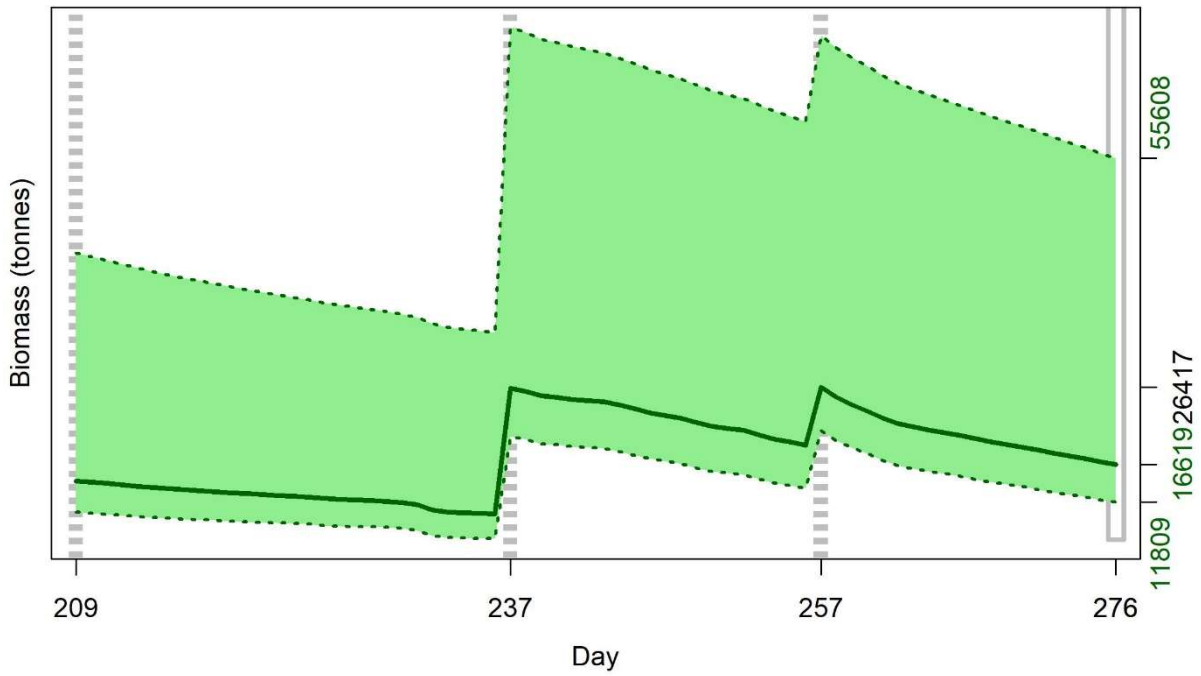

Figure 9 [previous page]. North sub-area. *D. gahi* biomass time series estimated from Bayesian posterior of the depletion model ± 95% confidence interval. Broken grey bars indicate the start of in-season depletions north; days 209, 237 and 257. Note that the biomass 'footprint' on day 276 (October 3rd) corresponds to the right-side plot of Figure 8.

On the first day of the season estimated *D. gahi* biomass north was 14,498 t ~ 95% CI [10,491 – 43,505] t; not statistically different from the pre-season estimate of 28,395 t [13,553 – 38,992] (Winter et al. 2022). The highest biomass estimate of the season occurred with the third immigration on day 257, reaching 26,417 t [20,896 – 71,169]. Effectively, the variation of biomass estimate throughout the season was not statistically significant; by the rule that a straight line could be drawn through the plot (Figure 9) without intersecting the 95% confidence interval (Swartzman et al. 1992).

Immigration

Doryteuthis gahi immigration during the season was inferred on each day by how many more squid were estimated present than the day before, minus the number caught and the number expected to have died naturally:

$$_{\text{Immigration}}N_{\text{day i}} = N_{\text{day i}} - (N_{\text{day i-1}} - C_{\text{day i-1}} - M_{\text{day i-1}})$$

where $N_{\text{day i-1}}$ are optimized in the depletion models, $C_{\text{day i-1}}$ calculated as in Equations **2** and **3**, and $M_{\text{day i-1}}$ is:

$$M_{\text{day i-1}} = (N_{\text{day i-1}} - C_{\text{day i-1}}) \times (1 - e^{-M})$$

Immigration biomass per day was then calculated as the immigration number per day multiplied by predicted average individual weight from the GAM:

$$_{\text{Immigration}}B_{\text{day i}} = {}_{\text{Immigration}}N_{\text{day i}} \times {}_{\text{GAM}}Wt_{\text{day i}}$$

All numbers N are themselves derived from the daily average individual weights, therefore the estimation automatically factors in that those squid immigrating on a given day would likely be smaller than average (because younger). Confidence intervals of the immigration estimates were calculated by applying the above algorithms to the MCMC iterations of the depletion models. Resulting total biomasses of *D. gahi* immigration north and south, up to season end (day 276), were:

$$_{\text{Immigration}}B_{\text{S season}} = 22{,}506 \text{ t} \sim 95\% \text{ CI } [12{,}679 \text{ to } 29{,}583] \text{ t} \quad \textbf{(9-S)}$$

$$_{\text{Immigration}}B_{\text{N season}} = 22{,}923 \text{ t} \sim 95\% \text{ CI } [16{,}736 \text{ to } 52{,}754] \text{ t} \quad \textbf{(9-N)}$$

Total immigration with semi-randomized addition of the confidence intervals was:

$$_{\text{Immigration}}B_{\text{Total season}} = 45{,}428 \text{ t} \sim 95\% \text{ CI } [37{,}113 \text{ to } 71{,}013] \text{ t} \quad \textbf{(9-T)}$$

In the south sub-area, the in-season peaks on days 215 and 270 accounted for approximately 65.6% and 29.1% of in-season immigration (start day 209 was de facto not an in-season

immigration). In the north sub-area, the in-season peaks on days 237 and 257 accounted for approximately 63.3% and 30.9% of in-season immigration. Both south and north, the remaining immigration percentages were accounted for by the minor fluctuations throughout the season.

Escapement biomass

Total escapement biomass was defined as the aggregate biomass of *D. gahi* at the end of day 276 (October 3rd) for south and north sub-areas combined (Equations **9**). Depletion models are calculated on the inference that all fishing and natural mortality are gathered at mid-day, thus a half day of mortality ($e^{-M/2}$) was added to correspond to the closure of the fishery at 23:59 (mid-night) on October 3rd for the final remaining vessels: Equation **10**.

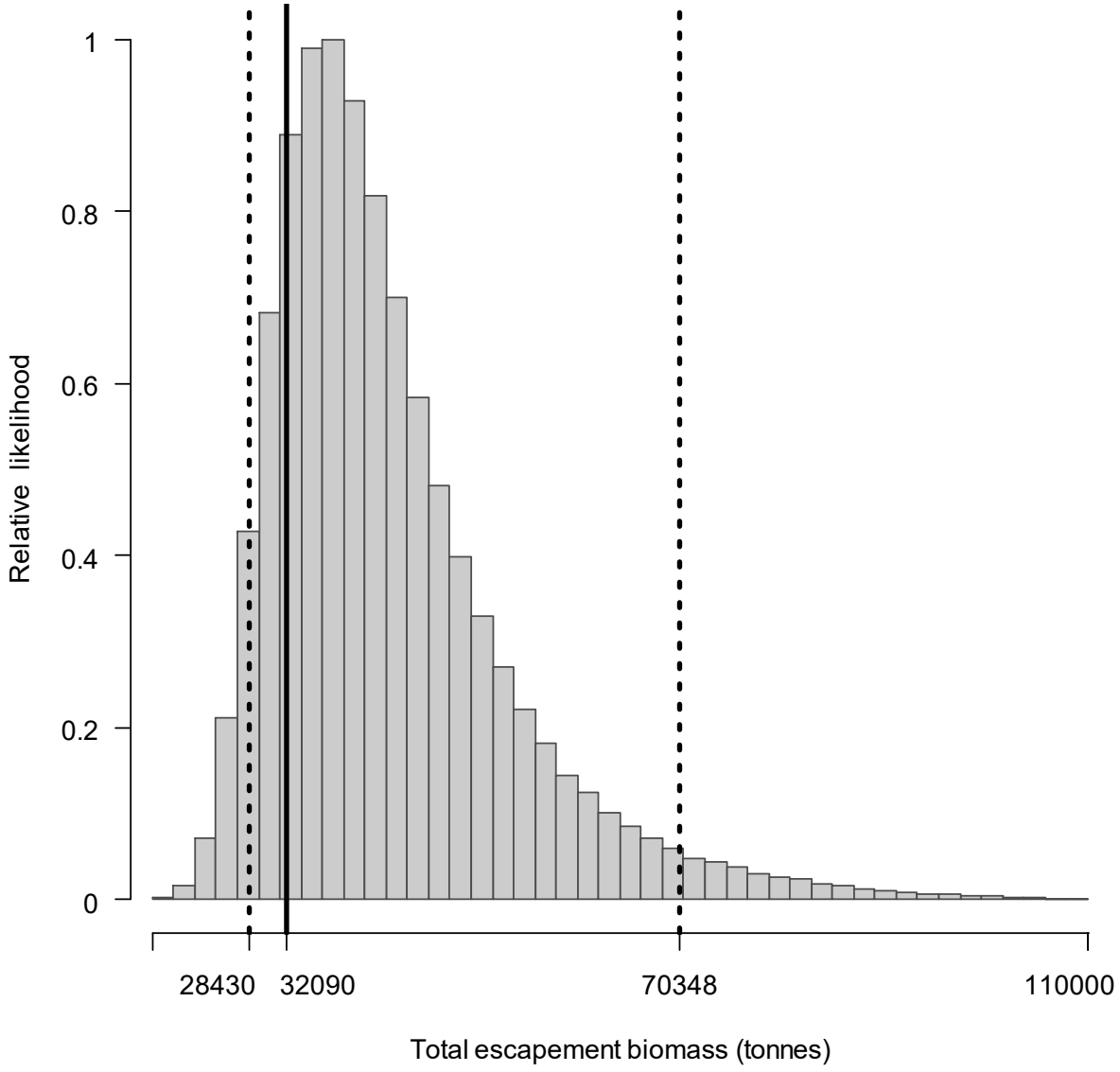

Figure 10. Likelihood distribution with 95% confidence interval of total *D. gahi* escapement biomass at the season end (October 3rd).

$$B_{\text{Total day 276}} = (B_{\text{S day 276}} + B_{\text{N day 276}}) \times e^{-M/2}$$

$$= 32{,}304 \text{ t} \times 0.99336$$

$$= 32{,}090 \text{ t} \sim 95\% \text{ CI } [26{,}920 - 73{,}086] \text{ t} \quad \textbf{(10)}$$

South and north biomass time series were negatively correlated: $R = -0.709$, $p < 0.001$. Randomized addition of the south and north distributions gave the aggregate likelihood of total escapement biomass ($B_{\text{Total day 276}}$) shown in Figure 10. The estimated escapement biomass of 32,090 t was the third-highest on record (since 2004) following 2018 and 2021. The risk of the fishery in the current season, defined as the proportion of the total escapement biomass distribution below the conservation limit of 10,000 tonnes (Agnew et al. 2002, Barton 2002), was effectively zero. For comparison, the minimum aggregate biomass of the season was estimated on day 269 (September 26th) as 28,512 t ~ 95% CI [23,527 – 70,551] t; also with zero risk of < 10,000 tonnes.

Fishery bycatch

All 982 second-season vessel-days (Table 1) reported *D. gahi* squid as their primary catch. The proportion of season total catch represented by *D. gahi* (43216202/43773741 = 0.987; Table A1) is highest for a 2nd season since 2019 and part of an increasing trend since about 12 years.

Figure 11 [below]. Distributions of the eight main bycatches during second season 2022, by noon position grids. Thickness of grid lines is proportional to the number of vessel-days (1 to 123 per grid; 23 different grids were occupied). Grey-scale is proportional to the season bycatch biomass per grid; maximum (tonnes) indicated on each plot.

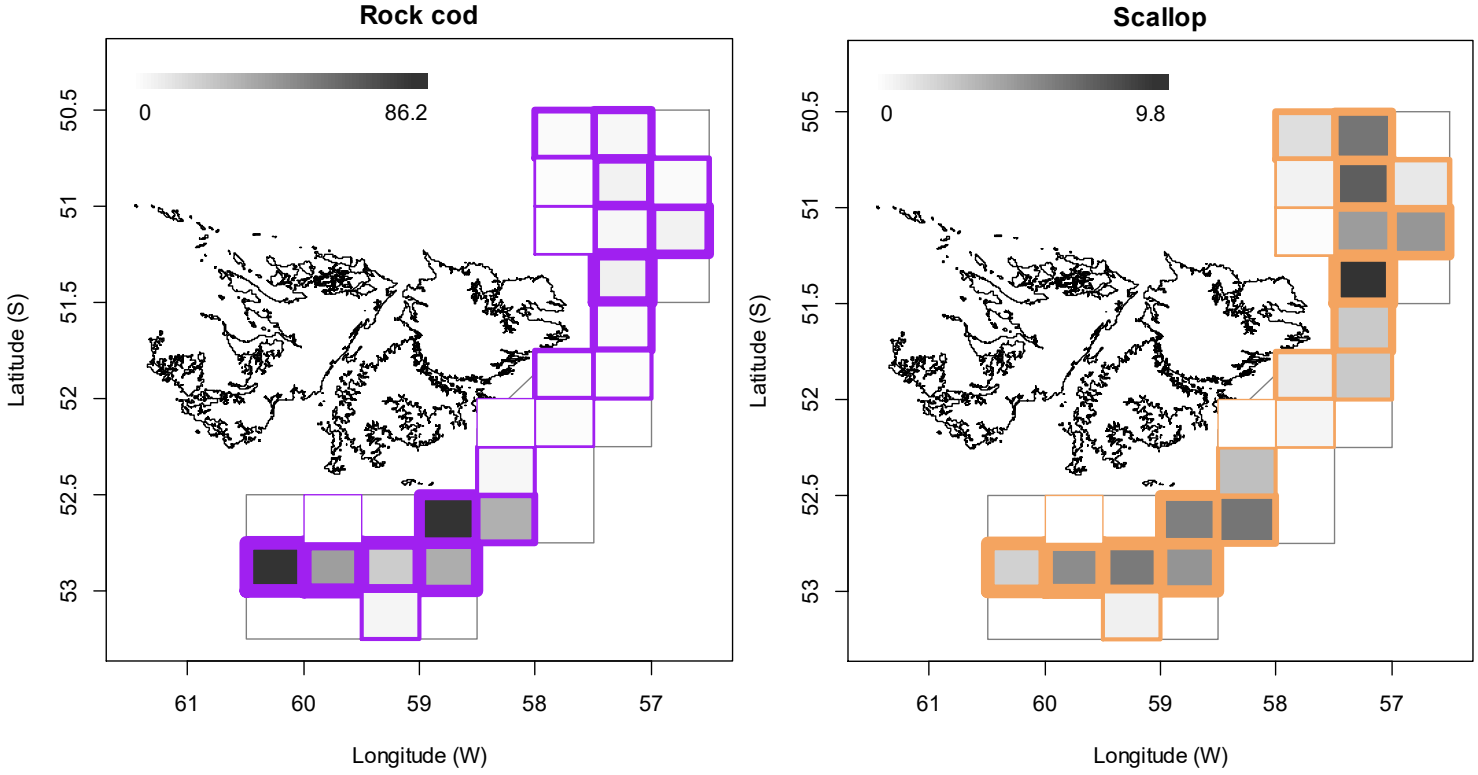

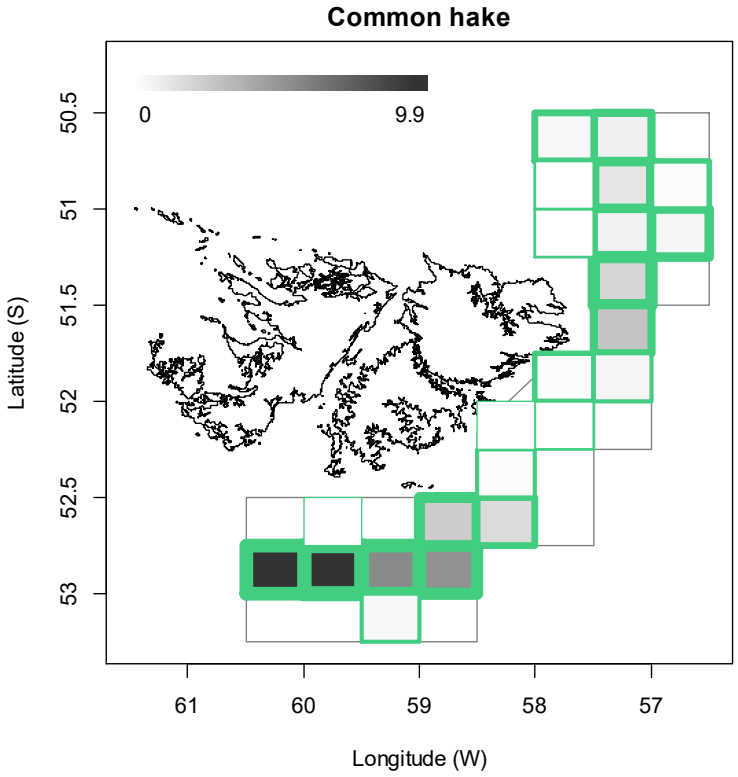
Common hake
0
9.9
Latitude (S)
50.5
51
51.5
52
52.5
53
61
60
59
58
57
Longitude (W)

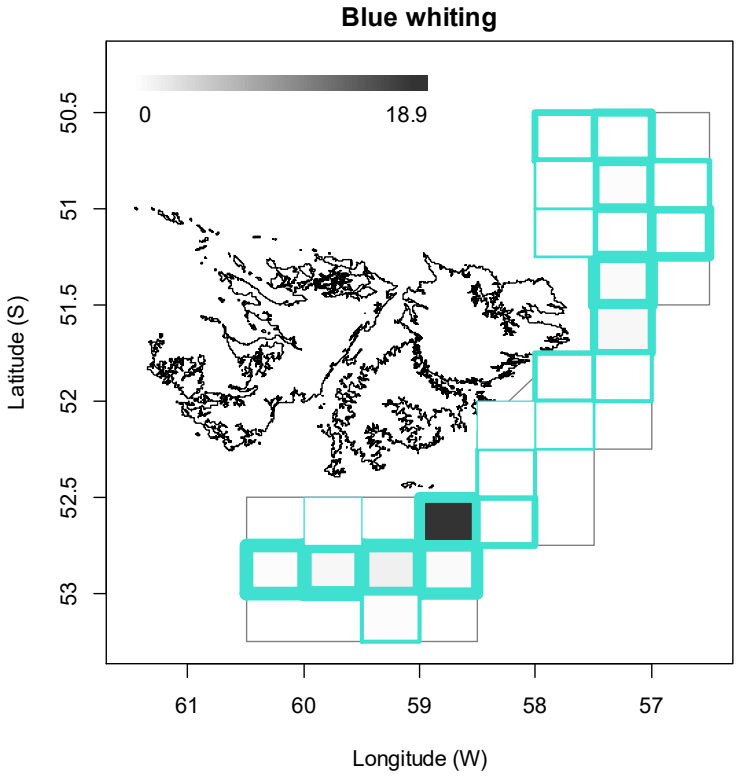
Blue whiting
0
18.9
Latitude (S)
50.5
51
51.5
52
52.5
53
61
60
59
58
57
Longitude (W)

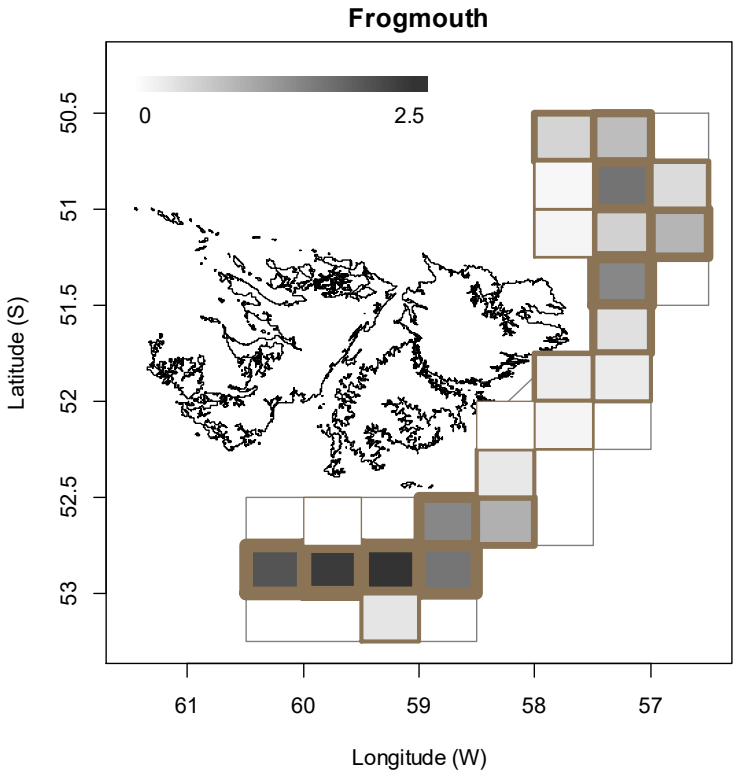
Frogmouth
0
2.5
Latitude (S)
50.5
51
51.5
52
52.5
53
61
60
59
58
57
Longitude (W)

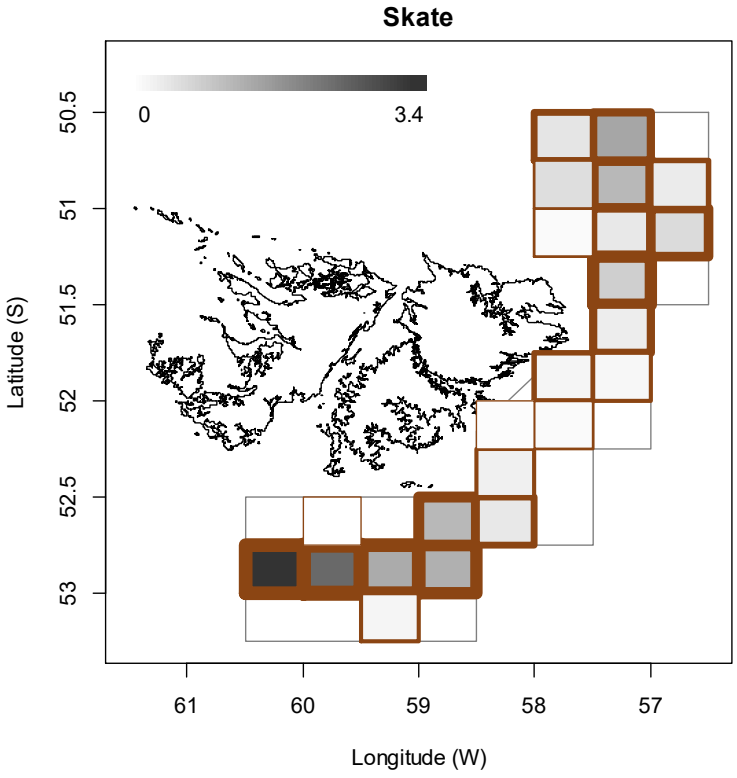
Skate
0
3.4
Latitude (S)
50.5
51
51.5
52
52.5
53
61
60
59
58
57
Longitude (W)

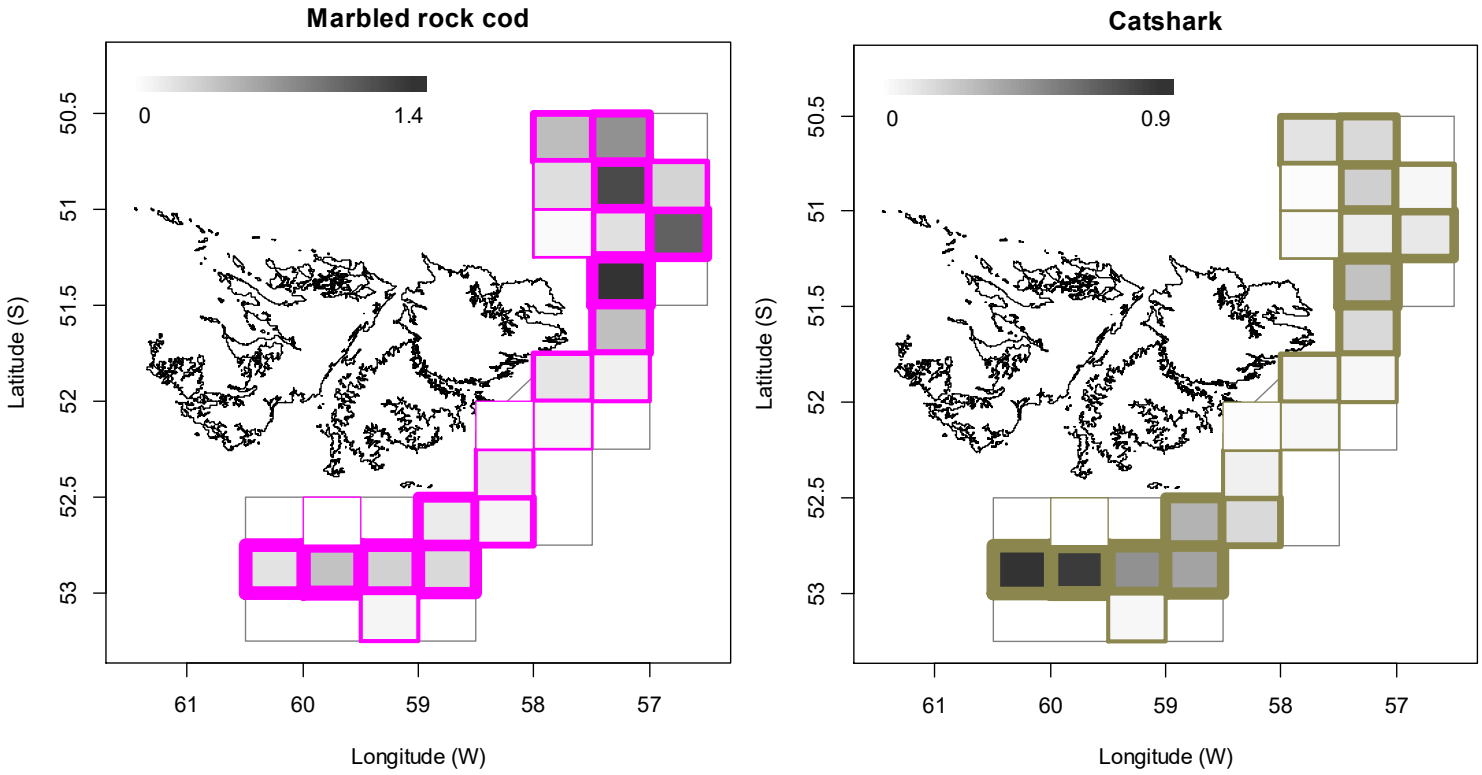

Highest aggregate bycatches in second season 2022 were common rock cod *Patagonotothen ramsayi* with 344 tonnes from 962 vessel-days (catch reports), scallops probably Zygochlamys (80 t, 746 v-days), common hake *Merluccius hubbsi* (45 t, 572 v-days), southern blue whiting *Micromesistius australis australis* (24 t, 81 v-days), frogmouth *Cottoperca gobio* (20 t, 870 v-days), skates Rajiformes (17 t, 824 v-days), marbled rock cod *Patagonotothen tessellata* (8 t, 262 v-days), and catshark *Schroederichthys bivius* (4 t, 552 v-days). Relative distributions by grid of these bycatches are shown in Figure 11; the complete list of all catches by species is in Table A1.

Trawl area coverage

The impact of bottom trawling on seafloor habitat has been a matter of concern in commercial fisheries (Kaiser et al. 2002; 2006), whereby the potential severity of impact relates to spatial and temporal extents of trawling (Piet and Hintzen 2012, Gerritsen et al. 2013), as well as the type of trawl gear (Rijnsdorp et al. 2020). For the *D. gahi* fishery, available catch, effort, and positional data are used to summarize the estimated 'ground' area coverage[c] occupied during the season of trawling.

The procedure for summarizing trawl area coverage is described in the Appendix of the second season 2019 report (Winter 2019). In second season 2022 50% of total *D. gahi* catch was taken from 2.8% of the total area of the Loligo Box, corresponding approximately[d] to the

[c] Appropriate spatial scale for calculating area coverage is a matter of some debate (Amoroso et al. 2018, Kroodsma et al. 2018). Given the comparatively small area of the Loligo Box, a high resolution of 5 km × 5 km was used for these calculations.

[d] However, not exactly. There is an expected strong correlation between the density of *D. gahi* catch taken from area units and how often these area units were trawled, but the correlation is not perfectly monotonic.

aggregate of grounds trawled ≥7.9 times. 90% of total *D. gahi* catch was taken from 12.7% of the total area of the Loligo Box, corresponding approximately to the aggregate of grounds trawled ≥2.5 times. 100% of total *D. gahi* catch over the season was taken from 19.5% of the total area of the Loligo Box, obviously corresponding to the aggregate of all grounds trawled at least once (Figure 12 - left). The 19.5% total trawl area coverage is highest among the nine seasons that have been given this analysis so far. Averaged by 5 × 5 km grid (Figure 12 - right), 10 grids (out of 1383) had coverage of 10 or more (that is to say, every patch of ground within that 5 × 5 km was on average trawled over 10 times or more). Fifty-seven grids had coverage of 5 or more, and 132 grids had coverage of 2 or more.

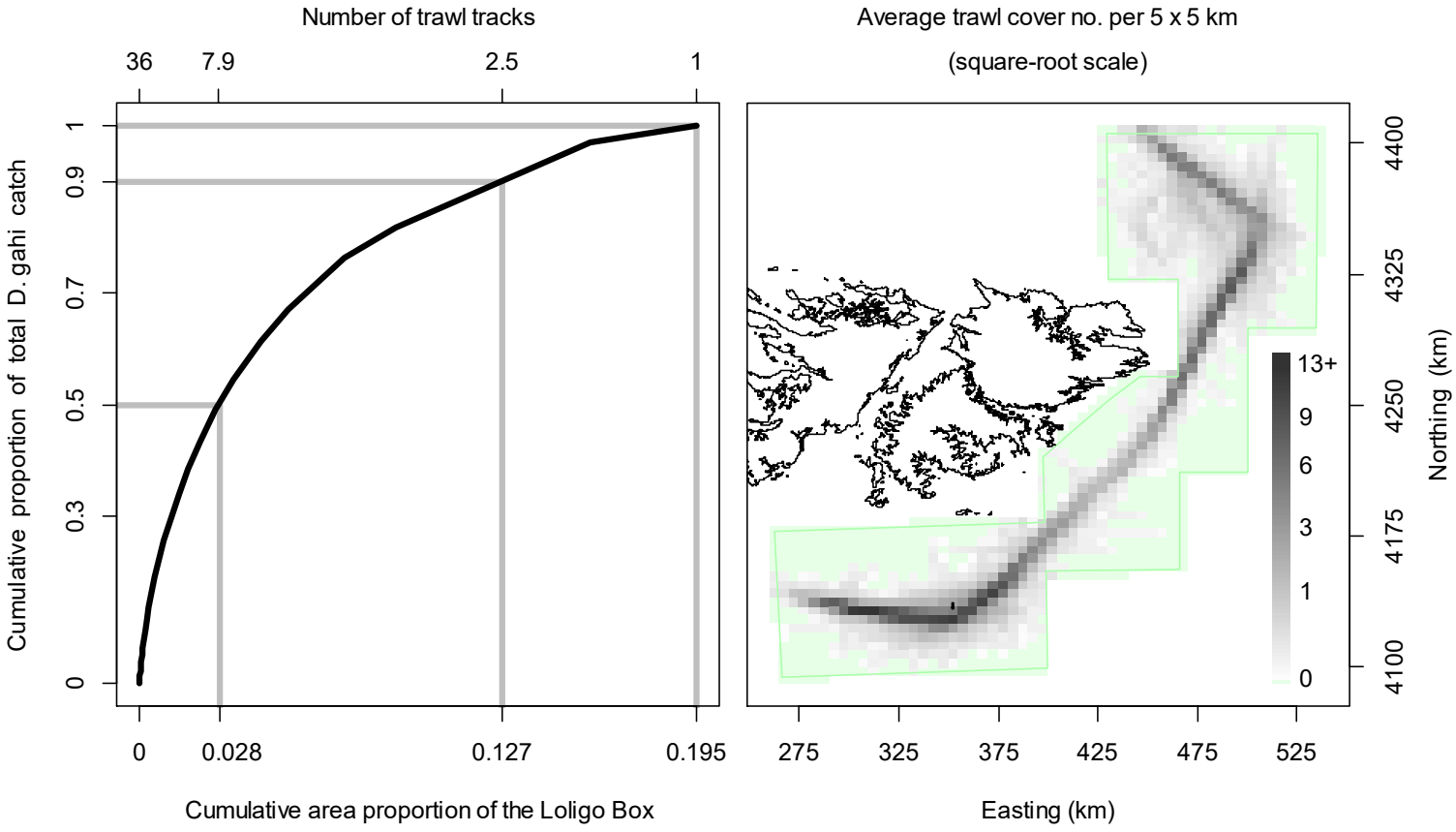

Figure 12. Left: cumulative *D. gahi* catch of 2nd season 2022, vs. cumulative area proportion of the Loligo Box the catch was taken from. The maximum number of times that any single area unit was trawled was 36, and catch cumulation by reverse density corresponded approximately to the trawl multiples shown on the top x-axis. Right: trawl cover averaged by 5 × 5 km grid; green area represents zero trawling.

References

Agnew, D.J., Baranowski, R., Beddington, J.R., des Clers, S., Nolan, C.P. 1998. Approaches to assessing stocks of *Loligo gahi* around the Falkland Islands. Fisheries Research 35: 155-169.

Agnew, D. J., Beddington, J. R., and Hill, S. 2002. The potential use of environmental information to manage squid stocks. Canadian Journal of Fisheries and Aquatic Sciences, 59: 1851–1857.

Akaike, H. 1973. Information theory and an extension of the maximum likelihood principle. 2nd International Symposium on Information Theory: 267-281.

Amoroso, R.O., Parma, A.M., Pitcher, C.R., McConnaughey, R.A., Jennings, S. 2018. Comment on "Tracking the global footprint of fisheries". Science 361: eaat6713.

Arkhipkin, A. 1993. Statolith microstructure and maximum age of *Loligo gahi* (Myopsida: Loliginidae) on the Patagonian Shelf. Journal of the Marine Biological Association of the UK 73: 979-982.

Arkhipkin, A.I., Middleton, D.A.J. 2002. Sexual segregation in ontogenetic migrations by the squid *Loligo gahi* around the Falkland Islands. Bulletin of Marine Science 71: 109-127.

Arkhipkin, A.I., Middleton, D.A.J., Barton, J. 2008. Management and conservation of a short-lived fishery resource: *Loligo gahi* around the Falkland Islands. American Fisheries Society Symposium 49: 1243-1252.

Arkhipkin, A.I., Hendrickson, L.C., Payá, I., Pierce, G.J., Roa-Ureta, R.H., Robin, J.-P., Winter, A. 2021. Stock assessment and management of cephalopods: advances and challenges for short-lived fishery resources. ICES Journal of Marine Science 78: 714-730.

Barton, J. 2002. Fisheries and fisheries management in Falkland Islands Conservation Zones. Aquatic Conservation: Marine and Freshwater Ecosystems 12: 127–135.

Brooks, S.P., Gelman, A. 1998. General methods for monitoring convergence of iterative simulations. Journal of computational and graphical statistics 7:434-455.

Carlson, J.E. 2014. A generalization of Pythagoras's theorem and application to explanations of variance contributions in linear models. Research Report No. RR-14-18, Princeton, NJ: Educational Testing Service. 17 p.

Copping, L. 2022. Observer Report 1336. Technical Document, FIG Fisheries Department. 27 p.

DeLury, D.B. 1947. On the estimation of biological populations. Biometrics 3: 145-167.

FIFD. 2004. Fishery Report, *Loligo gahi*, Second Season 2004. Fishing statistics, biological trends, and stock assessment. Technical Document, Falkland Islands Fisheries Department. 15 p.

Gamerman, D., Lopes, H.F. 2006. Markov Chain Monte Carlo. Stochastic simulation for Bayesian inference. 2nd edition. Chapman & Hall/CRC.

Gerritsen, H.D., Minto, C., Lordan, C. 2013. How much of the seabed is impacted by mobile fishing gear? Absolute estimates from Vessel Monitoring System (VMS) point data. ICES Journal of Marine Science 70: 523-531.

Hoenig, J. M. 1982. A compilation of mortality and longevity estimates for fish, mollusks, and cetaceans, with a bibliography of comparative life history studies. University of Rhode Island, Graduate School of Oceanography, Technical Report, 82-2. 14 p.

Hoenig, J.M. 1983. Empirical use of longevity data to estimate mortality rates. Fishery Bulletin 82: 898-903

Kaiser, M.J., Collie, J.S., Hall, S.J., Jennings, S., Poiner, I.R. 2002. Modification of marine habitats by trawling activities: prognosis and solutions. Fish and Fisheries 3: 114-136.

Kaiser, M.J., Clarke, K.R., Hinz, H., Austen, M.C.V., Somerfield, P.J., Karakassis, I. 2006. Global analysis of response and recovery of benthic biota to fishing. Marine Ecology Progress Series 311: 1-14.

Kroodsma, D.A., Mayorga, J., Hochberg, T., Miller, N.A., Boerder, K., Ferretti, F., Wilson, A., Bergman, B., White, T.D., Block, B.A., Woods, P., Sullivan, B., Costello, C., Worm, B. 2018. Response to Comment on "Tracking the global footprint of fisheries". Science 361: eaat7789.

Lipiński, M. R. 1979. Universal maturity scale for the commercially important squids (Cephalopoda: Teuthoidea). The results of maturity classification of *Illex illecebrosus* (Le Sueur 1821) population for years 1973–1977. ICNAF Research Document 79/11/38, 40 p.

MacCall, A.D. 2009. Depletion-corrected average catch: a simple formula for estimating sustainable yields in data-poor situations. ICES Journal of Marine Science 66: 2267-2271.

Magnusson, A., Punt, A., Hilborn, R. 2013. Measuring uncertainty in fisheries stock assessment: the delta method, bootstrap, and MCMC. Fish and Fisheries 14: 325-342.

Matosevic, N. 2022a. Observer Report 1333. Technical Document, FIG Fisheries Department. 22 p.

Matosevic, N. 2022b. Observer Report 1340. Technical Document, FIG Fisheries Department. 29 p.

Nash, J.C., Varadhan, R. 2011. optimx: A replacement and extension of the optim() function. R package version 2011-2.27. http://CRAN.R-project.org/package=optimx

Patterson, K.R. 1988. Life history of Patagonian squid *Loligo gahi* and growth parameter estimates using least-squares fits to linear and von Bertalanffy models. Marine Ecology Progress Series 47: 65-74.

Payá, I. 2006. Fishery Report. *Loligo gahi*, Second Season 2006. Fishery statistics, biological trends, stock assessment and risk analysis. Technical Document, Falkland Islands Fisheries Dept. 40 p.

Payá, I. 2010. Fishery Report. *Loligo gahi*, Second Season 2009. Fishery statistics, biological trends, stock assessment and risk analysis. Technical Document, Falkland Islands Fisheries Dept. 54 p.

Pierce, G.J., Guerra, A. 1994. Stock assessment methods used for cephalopod fisheries. Fisheries Research 21: 255–285.

Piet, G.J., Hintzen, N.T. 2012. Indicators of fishing pressure and seafloor integrity. ICES Journal of Marine Science 69: 1850-1858.

Plet-Hansen, K.S., Larsen, E., Mortensen, L.O., Nielsen, J.R., Ulrich, C. 2018. Unravelling the scientific potential of high-resolution fishery data. Aquatic Living Resources 31:24.

Punt, A.E., Hilborn, R. 1997. Fisheries stock assessment and decision analysis: the Bayesian approach. Reviews in Fish Biology and Fisheries 7:35-63.

Rijnsdorp, A.D., Hiddink, J.G., van Denderen, P.D., Hintzen, N.T., Eigaard, O.R., Valanko, S., Bastardie, F., Bolam, S.G., Boulcott, P., Egekvist, J., Garcia, C., van Hoey, G., Jonsson, P., Laffargue, P., Nielsen, J.R., Piet, G.J., Sköld, M., van Kooten, T. 2020. Different bottom trawl fisheries have a differential impact on the status of the North Sea seafloor habitats. ICES Journal of Marine Science 77: 1772–1786.

Roa-Ureta, R. 2012. Modelling in-season pulses of recruitment and hyperstability-hyperdepletion in the *Loligo gahi* fishery around the Falkland Islands with generalized depletion models. ICES Journal of Marine Science 69: 1403–1415.

Roa-Ureta, R., Arkhipkin, A.I. 2007. Short-term stock assessment of *Loligo gahi* at the Falkland Islands: sequential use of stochastic biomass projection and stock depletion models. ICES Journal of Marine Science 64: 3-17.

Rosenberg, A.A., Kirkwood, G.P., Crombie, J.A., Beddington, J.R. 1990. The assessment of stocks of annual squid species. Fisheries Research 8: 335-350.

Sadd, D. 2022. Observer Report 1334. Technical Document, FIG Fisheries Department. 16 p.

Shaw, P.W., Arkhipkin, A.I., Adcock, G.J., Burnett, W.J., Carvalho, G.R., Scherbich, J.N., Villegas, P.A. 2004. DNA markers indicate that distinct spawning cohorts and aggregations of Patagonian squid, *Loligo gahi*, do not represent genetically discrete subpopulations. Marine Biology, 144: 961-970.

Swartzman, G., Huang, C., Kaluzny, S. 1992. Spatial analysis of Bering Sea groundfish survey data using generalized additive models. Canadian Journal of Fisheries and Aquatic Sciences 49: 1366-1378.

Winter, A. 2019. Stock assessment – Falkland calamari *Doryteuthis gahi* 2nd season 2019. Technical Document, Falkland Islands Fisheries Department. 36 p.

Winter, A., Arkhipkin, A. 2015. Environmental impacts on recruitment migrations of Patagonian longfin squid (*Doryteuthis gahi*) in the Falkland Islands with reference to stock assessment. Fisheries Research 172: 85-95.

Winter, A., Arkhipkin, A., Matosevic, N., Copping, L. 2022. Falkland calamari (*Doryteuthis gahi*) 2nd pre-season 2022 stock assessment survey. Technical Document, Falkland Islands Fisheries Department. 17 p.

Appendix
***Doryteuthis gahi* individual weights**

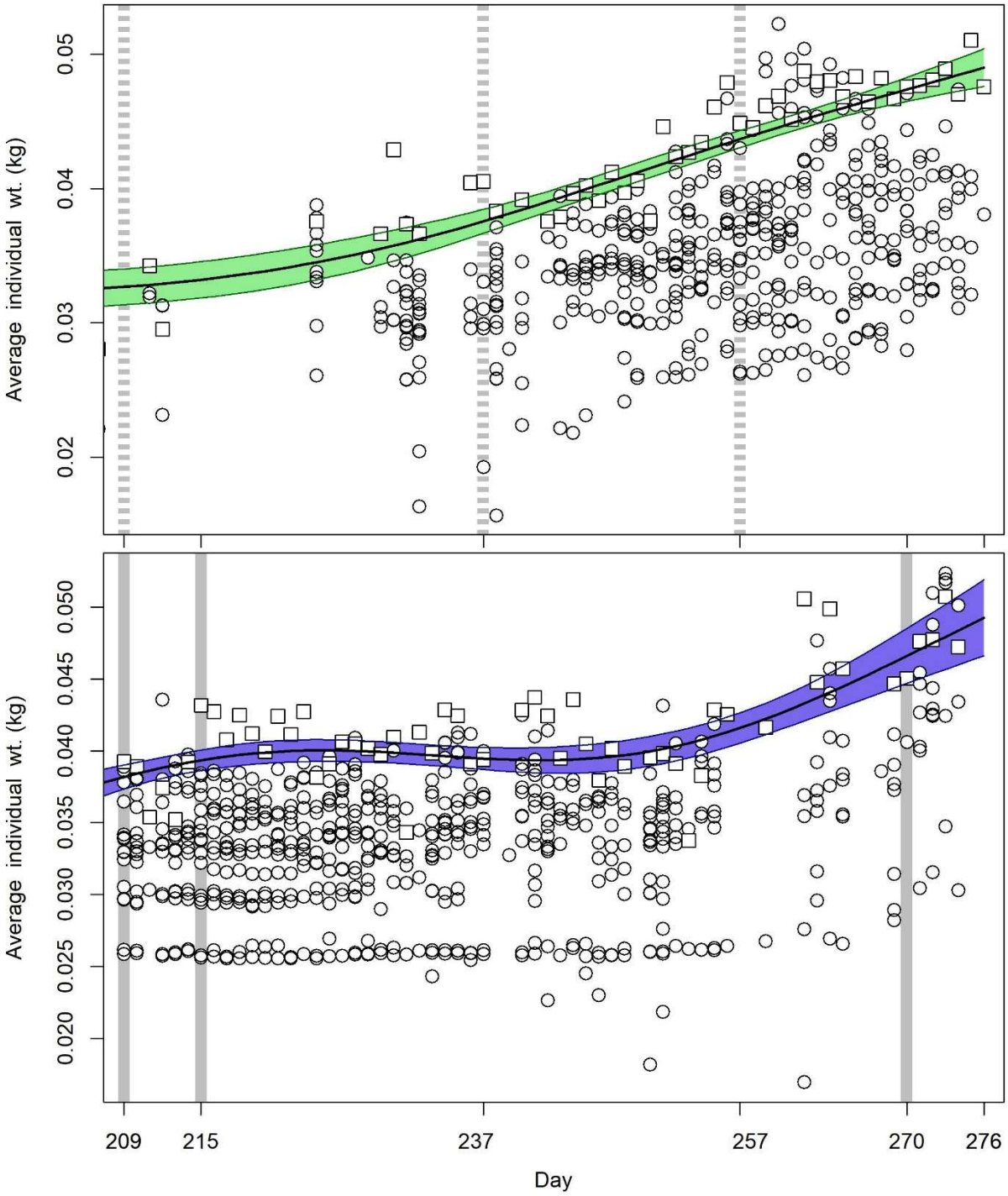

Figure A1. North (top) and south (bottom) sub-area daily average individual *D. gahi* weights from commercial size categories per vessel (circles) and observer measurements (squares). GAMs of the daily trends ± 95% confidence interval (centre lines and colour under-shading).

To smooth fluctuations, GAM trends were calculated of daily average individual weights. North and south sub-areas were calculated separately. For continuity, GAMs were calculated using all pre-season survey and in-season data contiguously. North and south GAMs were first

calculated separately on the commercial and observer data. As full observer coverage in the *D. gahi* fishery has now become standard, observer data GAMs were taken as the baseline trends, augmented by the margin by which commercial data are more frequent than observer data (if at all). For example, this season had 982 commercial fishing days (Table 1), and 894 observer days. The final GAM trend was therefore calculated as:

$$\mathrm{GAM_{Wt}} = \mathrm{Obs\ GAM_{Wt}} - \left(1 - \mathrm{pmin}\left(1, \frac{894}{982}\right)\right) \times \mathrm{mean}(\mathrm{Obs\ GAM_{Wt}} - \mathrm{Comm\ GAM_{Wt}})$$

As before, inclusion of both GAMs effected that the greater day-to-day consistency of the commercial data trends, and the greater point value accuracy of the observer data, are represented in the calculations. GAM plots of the north and south sub-areas are in Figure A1.

Prior estimates and CV

The pre-season survey had estimated *D. gahi* biomass of 63,348 tonnes (Winter et al. 2022). Hierarchical bootstrapping of the inverse distance weighting algorithm obtained a coefficient of variation (CV) equal to 14.9% of the survey biomass distribution. From modelled survey catchability, Payá (2010) had estimated average net escapement of up to 22%, which was added to the CV:

$$63{,}348 \pm (.149 + .22) = 63{,}348 \pm 36.9\% = 63{,}348 \pm 23{,}375 \text{ t} \quad \textbf{(A1)}$$

The 22% escapement was added as a linear increase in the variability, but was not used to reduce the total estimate, because squid that escape one trawl are likely to be part of the biomass concentration that is available to the next trawl.

D. gahi numbers from the survey were estimated as the survey biomasses divided by the GAM-predicted individual weight average for the survey: 0.0359 kg. The average coefficient of variation (CV) of the GAM over the duration of the pre-season survey was 1.9%, and CV of the length-weight conversion relationship (Equation **7**) was 9.8%. Joining these sources of variation with the pre-season survey biomass estimates and individual weight averages (above) gave estimated *D. gahi* numbers at survey end (day 207) of:

$$\begin{aligned} {}_{\text{prior}}\mathrm{N}_{\text{day 207}} &= \frac{63{,}348 \times 1000}{0.0359} \pm \sqrt{36.9\%^2 + 1.9\%^2 + 9.8\%^2} \\ &= 1.762 \times 10^9 \pm 38.2\% \end{aligned} \quad \textbf{(A2)}$$

The combined catchability coefficient (q) prior was taken on day 209, the first day of the season, when 15 vessels fished in the south sub-area and no vessels fished in the north sub-area (15 total; Figure 3). Abundance on day 209 was discounted for natural mortality over the 2 days since the end of the survey:

$${}_{\text{prior}}\mathrm{N}_{\text{day 209}} = {}_{\text{prior}}\mathrm{N}_{\text{day 207}} \times e^{-M\cdot(209-207)} - \mathrm{CNMD}_{\text{day 209}} = 1.716 \times 10^9 \quad \textbf{(A3)}$$

where $\mathrm{CNMD}_{\text{day 209}} = 0$ as no catches intervened between the end of the survey and the start of commercial season. Thus:

$${}_{\text{prior}}q = \mathrm{C(N)}_{\text{day 209}} / ({}_{\text{prior}}\mathrm{N}_{\text{day 209}} \times \mathrm{E}_{\text{day 209}})$$

$$= (C(B)_{\text{day 209}} / Wt_{\text{day 209}}) / ({}_{\text{prior}}N_{\text{day 209}} \times E_{\text{day 209}})$$

$$= (1450.0 \text{ t} / 0.0377 \text{ kg}) / (1.716 \times 10^{9} \times 15 \text{ vessel-days})$$

$$= 1.493 \times 10^{-3} \text{ vessels}^{-1} \text{ [e]} \qquad \textbf{(A4)}$$

$SD_{\text{prior q}}$ (Equation **4**) was calculated as ${}_{\text{prior}}q$ multiplied by its CV. $CV_{\text{prior q}}$ was calculated as the sum of variability in ${}_{\text{prior}}N_{\text{day 209}}$ (Equation **A2**) plus variability in the catches of vessels on start day 209, plus variability of the natural mortality (see Appendix section Natural mortality).

$$CV_{\text{prior q}} = \sqrt{38.2\%^2 + \left(\frac{SD\left(C(B)_{\text{vessels day 209}}\right)}{\text{mean}\left(C(B)_{\text{vessels day 209}}\right)}\right)^2 + (1 - (1 - CV_M)^{(209 - \text{mid\_survey})})^2}$$

$$= \sqrt{38.2\%^2 + 6.0\%^2 + 99.8\%^2} = 109.6\%$$

$$SD_{\text{prior q}} = {}_{\text{prior}}q \times CV_{\text{prior q}} = 1.637 \times 10^{-3} \text{ vessels}^{-1} \qquad \textbf{(A5)}$$

Depletion model estimates and CV

For the south sub-area, the equivalent of Equation **2** with three N_{day} was optimized on the difference between predicted and actual catches (Equation **3**), resulting in parameters values:

$${}_{\text{depletion}}N1_{S\text{ day 209}} = 0.829 \times 10^{9}; \quad {}_{\text{depletion}}N2_{S\text{ day 2015}} = 0.447 \times 10^{9}$$

$${}_{\text{depletion}}N3_{S\text{ day 270}} = 0.155 \times 10^{9}$$

$${}_{\text{depletion}}q_{S} = 2.190 \times 10^{-3} \text{ [f]} \qquad \textbf{(A6-S)}$$

The normalized root-mean-square deviation of predicted vs. actual catches was calculated as the CV of the model:

$$CV_{\text{rmsd S}} = \frac{\sqrt{\sum_{i=1}^{n}\left({}_{\text{predicted}}C(N)_{S\text{ day i}} - {}_{\text{actual}}C(N)_{S\text{ day i}}\right)^2 / n}}{\text{mean}\left({}_{\text{actual}}C(N)_{S\text{ day i}}\right)}$$

$$= 2.701 \times 10^{6} / 10.759 \times 10^{6} = 25.1\% \qquad \textbf{(A7-S)}$$

$CV_{\text{rmsd S}}$ was added to the variability of the GAM-predicted individual weight averages for the season (Figure A1-S); equal to a CV of 1.13% south. CVs of the depletion were then calculated as the sum:

$$CV_{\text{depletion S}} = \sqrt{CV_{\text{rmsd S}}^{\ 2} + CV_{\text{GAM Wt S}}^{\ 2}} = \sqrt{25.1\%^2 + 1.13\%^2}$$

$$= 25.1\% \qquad \textbf{(A8-S)}$$

[e] On Figure 6-left and Figure 8-left.
[f] On Figure 6-left.

For the north sub-area, the Equation **2** equivalent with three N_{day} was optimized on the difference between predicted and actual catches (Equation **3**), resulting in parameter values:

$$_{depletion}N1_{N\ day\ 209} = 1.313 \times 10^9; \quad _{depletion}N2_{N\ day\ 237} = 1.122 \times 10^9$$
$$_{depletion}N3_{N\ day\ 257} = 0.222 \times 10^9$$
$$_{depletion}q_{N} = 0.463 \times 10^{-3}\ ^{g} \qquad \textbf{(A6-N)}$$

Root-mean-square deviation of predicted vs. actual catches was calculated as the CV of the model:

$$CV_{\ rmsd\ N} = \frac{\sqrt{\sum_{i=1}^{n}\left({}_{predicted}C(N)_{N\ day\ i} - {}_{actual}C(N)_{N\ day\ i}\right)^2 / n}}{mean\left({}_{actual}C(N)_{N\ day\ i}\right)}$$

$$= 3.299 \times 10^6 / 10.759 \times 10^6 = 67.3\% \qquad \textbf{(A7-N)}$$

$CV_{rmsd\ N}$ was added to the variability of the GAM-predicted individual weight averages for the season (Figure A1-N); equal to a CV of 1.02% north. CVs of the depletion were then calculated as the sum:

$$CV_{\ depletion\ N} = \sqrt{CV_{\ rmsd\ N}{}^2 + CV_{\ GAM\ Wt\ N}{}^2} = \sqrt{67.3\%^2 + 1.02\%^2}$$
$$= 67.4\% \qquad \textbf{(A8-N)}$$

Combined Bayesian models

For the south sub-area, joint optimization of Equations **3** and **4** resulted in parameters values:

$$_{Bayesian}N1_{S\ day\ 209} = 0.884 \times 10^9; \quad _{Bayesian}N2_{S\ day\ 215} = 0.433 \times 10^9$$
$$_{Bayesian}N3_{S\ day\ 270} = 0.161 \times 10^9;$$
$$_{Bayesian}q_{S} = 2.043 \times 10^{-3}\ ^{h} \qquad \textbf{(A9-S)}$$

These parameters produced the fit between predicted catches and actual catches shown in Figure A2-S.

For the north sub-area, joint optimization of Equations **3** and **4** resulted in parameters values:

$$_{Bayesian}N1_{N\ day\ 209} = 0.444 \times 10^9; \quad _{Bayesian}N2_{N\ day\ 237} = 0.430 \times 10^9$$
$$_{Bayesian}N3_{N\ day\ 257} = 0.194 \times 10^9$$
$$_{Bayesian}q_{N} = 1.412 \times 10^{-3}\ ^{i} \qquad \textbf{(A9-N)}$$

These parameters produced the fit between predicted catches and actual catches shown in Figure A2-N.

[g] On Figure 8-left.
[h] On Figure 6-left.
[i] On Figure 8-left.

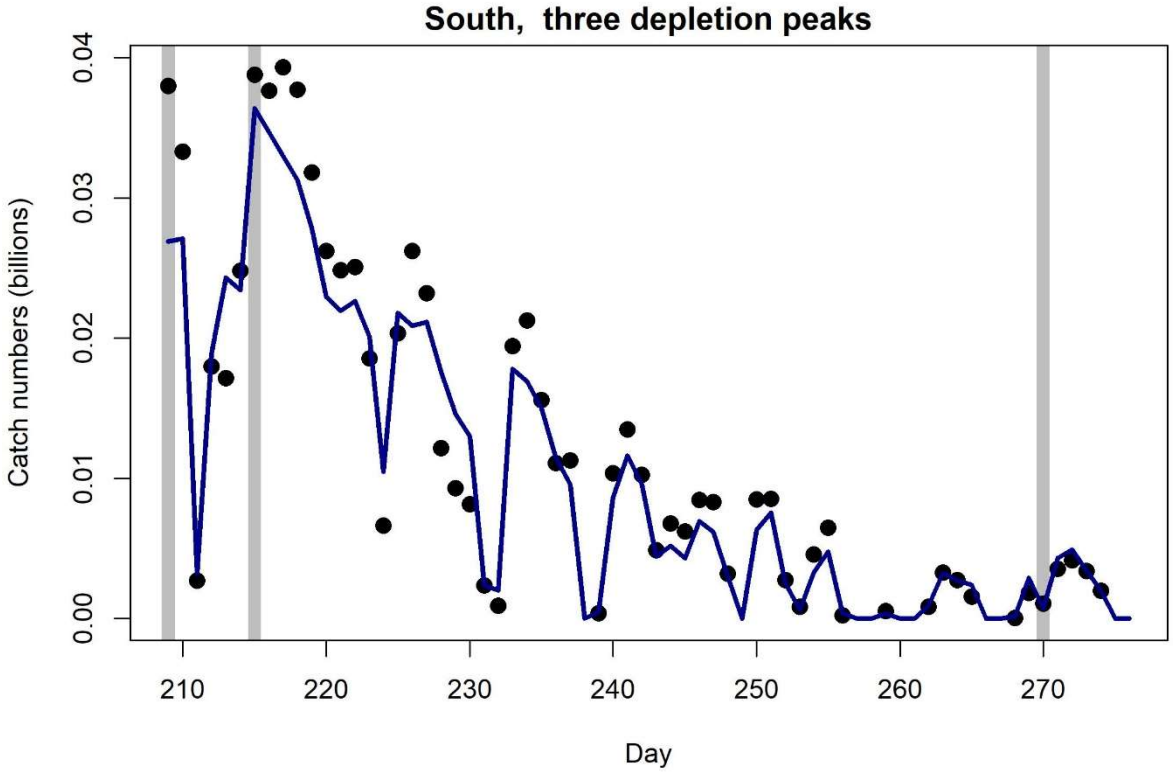

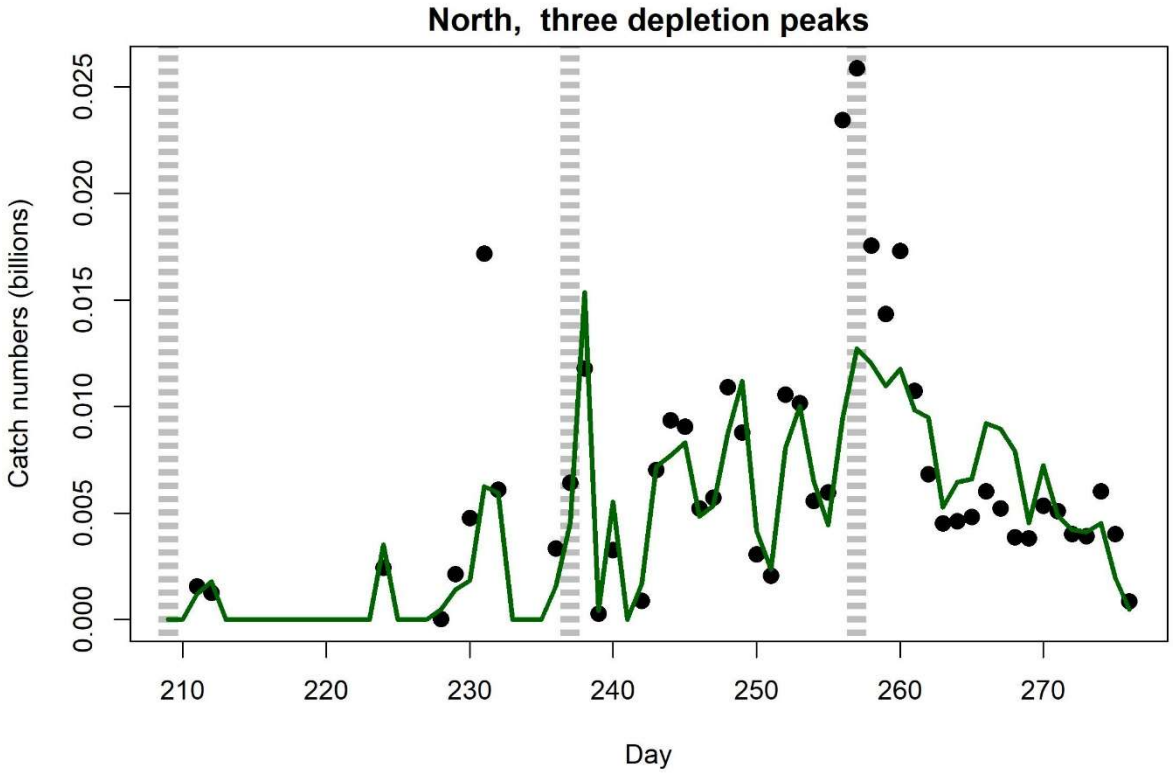

Figure A2-S [top]. Daily catch numbers estimated from actual catch (black points) and predicted from the depletion model (purple line) in the south sub-area.

Figure A2-N [bottom]. Daily catch numbers estimated from actual catch (black points) and predicted from the depletion model (green line) in the north sub-area.

Natural mortality

Natural mortality is parameterized as a constant instantaneous rate M = 0.0133 day^{-1} (Roa-Ureta and Arkhipkin 2007), based on Hoenig's (1983) log mortality vs. log maximum age regression, applied to an estimated maximum age of 352 days for *D. gahi*:

$$\log(M) = 1.44 - 0.982 \times \log(age_{max})$$

$$M = \exp(1.44 - 0.982 \times \log(352))$$

$$= 0.0133 \quad \textbf{(A10)}$$

Hoenig (1983) derived Equation **A10** from the regression of 134 stocks among 79 species of fish, molluscs, and cetaceans. Hoenig's regression obtained $R^2 = 0.82$, but a corresponding coefficient of variation (CV) was not published. In previous stock assessments (since Winter (2017)) an approximate CV of M was estimated by measuring the coordinates off a print of Figure 1 in Hoenig (1983) and randomly resampling the regression. CV estimation has now been revised by re-computing the regression from original data in Hoenig (1982)[j], extracting the standard error (σ), and calculating the CV from the equation:

$$CV = (\exp(\sigma^2) - 1)^{1/2} \quad \text{(MacCall 2009)}$$

which gave

$$CV_M = (\exp(0.472^2) - 1)^{1/2} = 49.96\% \quad \textbf{(A11)}$$

MacCall (2009) suggested that CV_M should be assumed a minimum of 0.5, effectively equivalent to Equation **A11**.

CV_M was aggregated over the number of days between the midpoint of the survey and the commercial season start, rather than between the end of the survey and commercial season start, as the midpoint more accurately reflects how much time has elapsed since the fishing area on average was surveyed. The midpoint of the survey was calculated as the mean day weighted by the number of survey trawls taken per day:

$$\text{mid\_survey} = \frac{\Sigma\left(\text{day} \times N_{\text{survey trawls}}|_{\text{day}}\right)}{\Sigma\left(N_{\text{survey trawls}}|_{\text{day}}\right)} = 200^{k}$$

(A12)

CV_M was thus further indexed by $1 - (1 - CV_M)$ to ensure that the value could not decrease if CV_M was hypothetically > 100%:

$$1 - (1 - CV_M)^{(\text{commercial season start} - \text{mid\_survey})} \quad \textbf{(A13)}$$

Equation **A13** is included in Equation **A5**.

[j] Hoenig (1982) listed 130 rather than 134 stocks, but these obtained the same regression parameters of 1.44 and –0.982.

[k] In common nomenclature day 200 is July 19th.

Biomass projection

Projecting *D. gahi* biomass forward, i.e., in-season beyond the last day of data received from the fishery, was carried out in three steps: 1) separately project CPUE, effort and average individual weight time-series into the future (this example posits a 7-day projection period), 2) calculate projected catch from projected CPUE and effort, and 3) concatenate the realized + projected time-series of catch, effort and average individual *D. gahi* weights to fit the depletion model and calculate projected biomass. The depletion model fitting procedure is then identical to the procedure used regularly during the season on realized data only (see Methods section), the difference being that realized + projected data are now fit jointly. For example, if the season started on day 209 and reached day 265, the depletion model would be fit to the concatenated time series of realized data from days 209-265 and projected data for days 266-272.

Two assumptions are required for this procedure:

- No further immigration will happen during the projection period. Future immigration cannot realistically be predicted from the accrued season data (or from past seasons), and therefore cannot be meaningfully included in the projection. As such, assuming no further immigration makes the projection conservative, allowing fishing companies to plan for potential worst-case scenarios.
- Effort will remain similar to what was observed prior to the projection. Effort can be actively changed by the FIFD (e.g. closing the south sub-area would lead to zero effort in the south and maximum effort in the north), or by the fishing industry (companies can decide to direct vessels from one area to another). Obviously, major changes in effort will void any projection that has not anticipated them, and therefore these changes cannot be included in the procedure.

CPUE, effort, average individual weight, and catch data were projected according to the following approaches:

- CPUE was projected by fitting a GAM (with gamma error distribution and canonical log-link) to the realized time-series of CPUE data, starting from the most recent immigration peak as the depletion curve currently in effect. The GAM fit was extrapolated for the required number of days forward, and potential future CPUE observations were simulated from the variability spread corresponding to the fitted model (Figure A3-A). A gamma error distribution was used because CPUE data consisted of positive, non-zero, values; very similar results were obtained when a lognormal error distribution was used instead.
- Effort was projected by sampling with replacement from the realized effort in a selected 'reference' period. The reference period was chosen ad-hoc, based on visual examination of trends in effort, with the aim of making the projected effort consistent with recently realized effort. In the current example, the reference period was set to capture the most recent change to lower levels of effort (Figure A3-B). Developing a more objective way of projecting effort remains a topic for future work.
- Average individual weight was projected by extrapolating the GAM fitted to the realized average individual weight time-series (Figure A3-C). Because the depletion model uses the optimal-fitted GAM values of average individual weight without error distribution, there was also no need to simulate projected average individual weights with variability (unlike the CPUE projections). Conceptually, average individual weights can be projected relatively reliably – without new immigration, average squid sizes should increase over time following a predictable trajectory.
- Catch was projected by multiplying projected CPUE × projected effort (Figure A3-D).

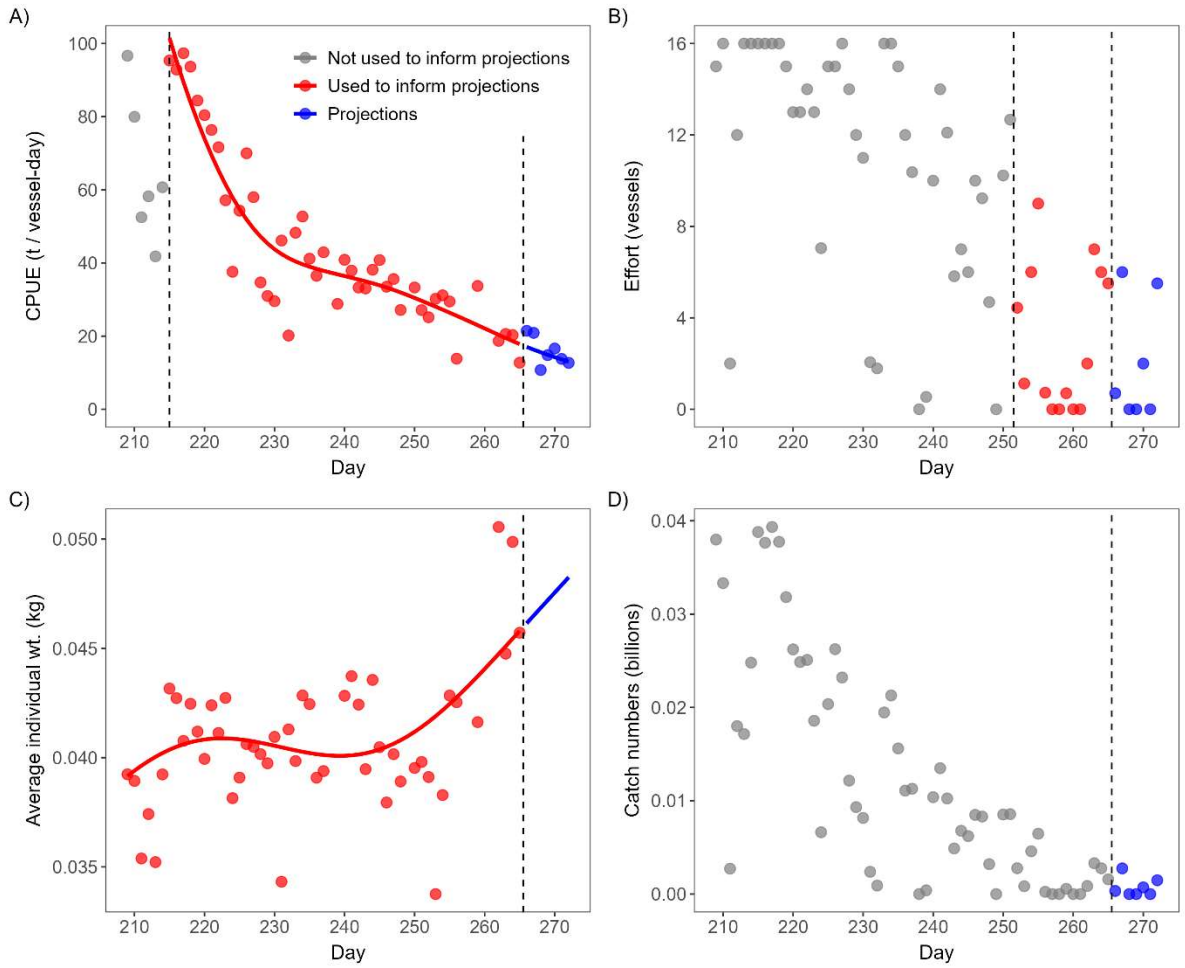

Figure A3. Realized (grey and red) and projected data/fits (blue) used in the depletion model to obtain biomass projections. A) GAM fit (red line) to the realized CPUE time-series (red dots) between the most recent immigration event (day 215, the first dashed line) and the start of the projection period (day 266, the second dashed line); the extrapolated GAM fit and projected daily CPUEs are shown as blue line and dots, respectively. B) Realized effort (red dots) during the ad-hoc selected period (days 252-265, between dashed lines) and the projected effort (blue dots). C) GAM fit (red line) to average individual weights (red dots) and the projected average individual weight (blue line). D) Projected catches (blue dots), calculated by multiplying projected CPUE and effort.

With CPUE, effort, average individual weight, and catch data projected seven days forward, the depletion model was fitted to the joint realized + projected data, and the biomass estimate was recalculated for the entire period; from the start of the season until the end of the projection period. Note that every recalculation of a depletion model is always holistic, i.e., the model re-estimates biomass on every day of the time series. The recalculation is not incremental, i.e., only biomass on the 'new' days is estimated. Thus, a projected depletion model can potentially give values that do not appear intuitive, as the early part of the time series is now calculated higher or lower than previously.

Uncertainty of the biomass projection was estimated by iterating 1000× the CPUE projection (random simulations of CPUE from the fitted GAM) and 1000× the effort projection (random draws with replacement in the selected 'reference' period), then depletion-modelling the projected biomass time series from each iteration (Figure A4; the 1000 iterations are

summarized as box plots per day). The probability of biomass falling below the conservation threshold was calculated for each day of the projection period as the proportion of the 1000 time-series estimates below the conservation threshold.

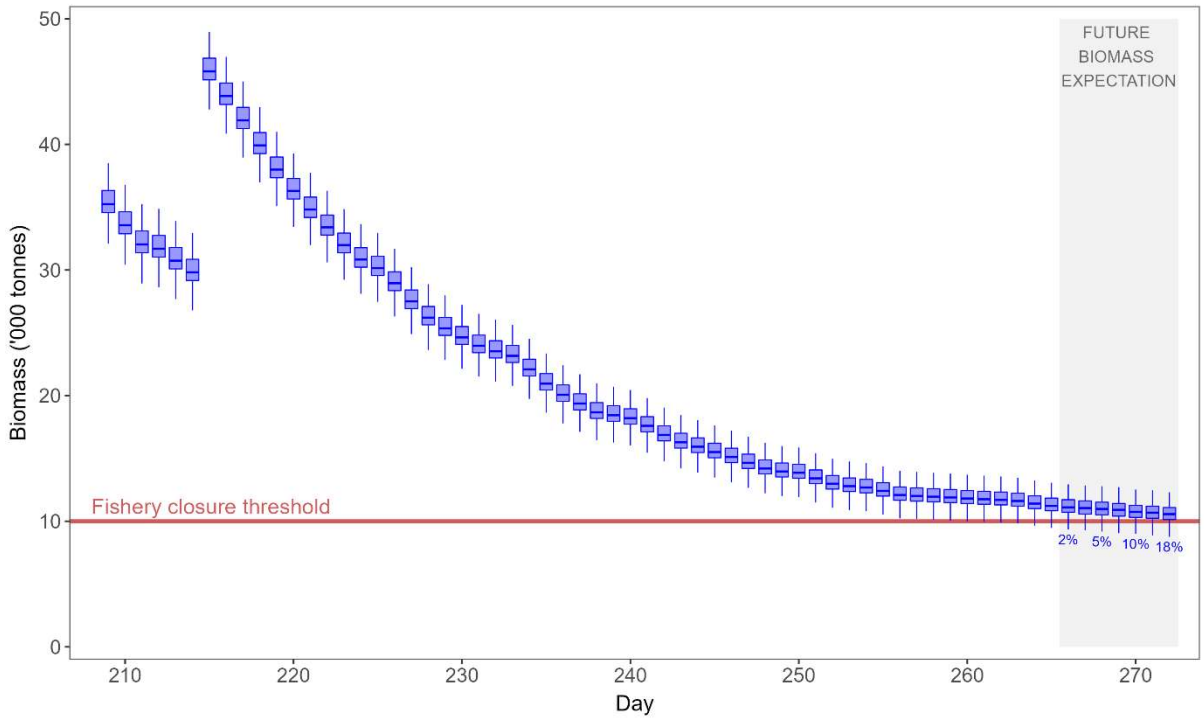

Figure A4. Projected biomass series, calculated from joint realized data on days 209-265 + projected data on days 266-272. The discontinuity in biomass time-series on day 215 is due to an immigration event. Percentages denote probability of biomass falling below conservation threshold on sequential days of the projection period.

The procedure described above applies to biomass projection over one sub-area, in this case the Loligo Box south of 52°S. For projection over the entire Loligo Box, the procedure is replicated over the sub-area north of 52°S. Iterations of south and north sub-area biomass projections are calculated in parallel, as they share the pool of effort: on any day the total effort cannot exceed 16 vessels, which is therefore partitioned between the two sub-areas. Parallel iterations of the south and north biomass projections are then added together for the total of 1000 projections to evaluate against the conservation threshold.

Total catch by species

Table A1: Total reported catches and discard by taxon during second season 2022 X-license fishing, and number of catch reports (vessel-days) in which each taxon occurred. Does not include incidental catches of pinnipeds or seabirds.

Species Code	Species / Taxon	Catch Wt. (KG)	Discard Wt. (KG)	N Reports
LOL	*Doryteuthis gahi*	43216202	79519	982
PAR	*Patagonotothen ramsayi*	343929	343929	962
SCA	Scallop	79586	79631	746
HAK	*Merluccius hubbsi*	44755	13165	572
BLU	*Micromesistius australis*	23503	11349	81
CGO	*Cottoperca gobio*	19586	19586	870
RAY	Rajidae	17058	16862	824
PTE	*Patagonotothen tessellata*	8092	8092	262
DGH	*Schroederichthys bivius*	4422	4422	552
SAR	*Sprattus fuegensis*	3720	3720	101
ING	*Moroteuthis ingens*	3174	3174	339
MED	Medusae sp.	2148	2148	102
LIM	*Lithodes murrayi*	1905	1905	146
LIT	*Lithodes turkayi*	838	838	74
OCT	*Octopus* spp.	831	831	156
MYX	*Myxine* spp.	678	678	104
UCH	Sea urchin	659	659	78
TOO	*Dissostichus eleginoides*	555	555	146
ILL	*Illex argentinus*	413	413	59
BAC	*Salilota australis*	337	337	65
SAA	*Salmo trutta*	304	304	11
KIN	*Genypterus blacodes*	266	256	42
MUL	*Eleginops maclovinus*	163	163	45
EEL	*Iluocoetes fimbriatus*	145	145	48
SPN	Porifera	115	115	4
GRC	*Macrourus carinatus*	88	88	3
GRV	*Macrourus* spp.	66	66	18
RED	*Sebastes oculatus*	50	50	11
MUN	*Munida* spp.	37	37	4
WHI	*Macruronus magellanicus*	36	36	4
NEM	*Neophyrnichthys marmoratus*	21	21	8
DGS	*Squalus acanthias*	20	20	1
PYM	*Physiculus marginatus*	17	17	1
MXX	Myctophid spp.	5	5	1
PAT	*Merluccius australis*	5	5	3
GRF	*Coelorhynchus fasciatus*	5	5	1
BUT	*Stromateus brasiliensis*	2	2	1
CHE	*Champsocephalus esox*	1	1	1
SEP	*Seriolella porosa*	1	1	1
ICA	*Icichthys australis*	1	1	1
NOW	*Paranotothenia magellanica*	1	1	1
COP	*Congiopodus peruvianus*	1	1	1
Total		43773741	593153	982